On Secure NOMA-Aided Semi-Grant-Free Systems

Hongjiang Lei, Fangtao Yang, Hongwu Liu, Imran Shafique Ansari,
Kyeong Jin Kim, and Theodoros A. Tsiftsis

Abstract

Semi-grant-free (SGF) transmission scheme enables grant-free (GF) users to utilize resource blocks allocated for grant-based (GB) users while maintaining the quality of service of GB users. This work investigates the secrecy performance of non-orthogonal multiple access (NOMA)-aided SGF systems. First, analytical expressions for the exact and asymptotic secrecy outage probability (SOP) of NOMA-aided SGF systems with a single GF user are derived. Then, the SGF systems with multiple GF users and the best-user scheduling scheme is considered. By utilizing order statistics theory, analytical expressions for the exact and asymptotic SOP are derived. Monte Carlo simulation results are provided and compared with two benchmark schemes. The effects of system parameters on the SOP of the considered system are demonstrated and the accuracy of the developed analytical results is verified. The results indicate that both the outage target rate for GB and the secure target rate for GF are the main factors of the secrecy performance of SGF systems.

Index Terms

Non-orthogonal multiple access (NOMA), semi-grant-free (SGF) transmission scheme, grant-free (GF) user, grant-based (GB) user, secrecy outage probability.

I. INTRODUCTION

A. Background and Related Work

Ultra-reliable low latency communications (URLLC) and massive machine-type communications (mMTC) are the two most important scenarios for the next internet of things (IoT). URLLC focuses on mission-critical applications wherein unprecedented levels of reliability and latency

are of the utmost importance in the fifth generation and it's beyond [1]. In contrast, mMTC aspires to connect a vast number of intelligent devices to the Internet. The user initiates the traditional grant-based (GB) access scheme with an access request to the base station (BS) in long term evolution. The BS responds by allocating an access grant through a four-step handshake procedure strategy. Once the BS grants the access request, data packets can be successfully transmitted without collision under ideal channel conditions. However, GB scheme does not suit these scenarios due to high latency and heavy signaling overhead [2], [3]. Moreover, the initial request transmission is still subject to collision and could require multiple transmissions depending on traffic load and the available resources at the BS.

To tackle these issues, grant-free (GF) transmission schemes were introduced in [4], [5], in which multiple users may occupy the same resource without the initial access request procedure. Unlike the GB principle, no dedicated request transmission for granting access and allocating resource blocks is required for GF communications before starting a data transmission. Although the GF scheme makes it possible to allow users to choose resource blocks independently and transmit data directly to reduce signaling overhead and latency effectively, collisions will become severe when multiple users select the same resource block to transmit simultaneously [6]. The collision issue can be resolved using massive multiple-input multiple-output (MIMO) or non-orthogonal multiple access (NOMA) technologies. The former solution utilizes spatial degrees of freedom to mitigate multi-user collisions, while the latter focuses on spectrum sharing among multiple users with successive interference cancellation (SIC) [7], [8], [9], [10].

Even though the massive connectivity can be supported through GF schemes, GB schemes are still desired, especially when strict quality of service (QoS) requirements exist [10]. The GB and GF transmission scheme must coexist in scenarios where URLLC applications are served by the GB scheme and mMTC applications in the same system are served by the GF scheme. For example, a new hybrid access scheme was proposed in [11] to meet the various requirements of IoT networks wherein machine-type users with small data packets and delay-tolerant traffic utilized the GF scheme, and some users with large data packets and delay-sensitive traffic used the GB scheme. NOMA-aided Semi-GF (SGF) transmission scheme was first explicitly introduced in [12] to alleviate the collisions and obtain massive connectivity. A single GB user with multiple GF users to perform NOMA and two contention control mechanisms were proposed to suppress the interference on the GB user from the GF users. Closed-form expressions for the outage probability (OP) of GF users were derived and the impact of different SIC decoding orders

was investigated. Their results demonstrated the superior performance of NOMA-aided SGF schemes. Based on the relationship between the GB user's targeted rate and channel conditions, an adaptive power allocation strategy was proposed to control the transmit power of GB users to ensure that the GB user's signals are always decoded in the second stage of SIC [13]. In [14], the authors investigated the performance of an uplink SGF system with multiple uniformly distributed GF and GB users considered, in which the GF user whose received power is lower at the BS than that of the GB user was selected to pair with the connected GB user. Closed-form expressions for GB and GF users' exact and approximate ergodic rates were derived. Further, the authors in [15] studied the effect of random locations of GF users on the performance of NOMA-assisted SGF systems by utilizing stochastic geometry. A dynamic threshold protocol was proposed to reduce the interference to GB users, and the outage performance was analyzed and compared with the open-loop protocol.

Relative to the SGF schemes proposed in [12], a new QoS-guarantee scheme for NOMA-aided SGF systems was proposed in [16] to ensure that the QoS of the GB user is the same as that when it solely occupies the channel. Closed-form expressions were derived for the exact and asymptotic OP with the best-user scheduling (BUS) scheme and a hybrid SIC scheme. The results demonstrated that the proposed scheme could significantly improve the reliability of the GF users' transmissions. Based on [16], a new adaptive power control strategy was proposed to solve OP error floors entirely by adjusting the GF user's transmit power to change the decoding order of SIC in [17]. In [18], the authors analyzed the outage performance of the NOMA-aided SGF systems with multiple randomly distributed GF users with fixed power and dynamic power schemes. As discussed in [18], the BUS scheme may lead to a fairness problem because the users closer to the base station may be scheduled more frequently due to weak path loss. To solve the fairness problem, a cumulative distribution function (CDF)-based user scheduling (CUS) scheme was proposed where the GF user with the maximal CDF value will be admitted to the channel. The analytical expressions for the OP with the CUS and BUS schemes were derived and the impacts of small-scale fading, path loss, and random user locations were jointly investigated.

Recently, physical layer security for NOMA systems has attracted considerable attention [19] - [26]. In [19], the authors investigated the secrecy performance of NOMA systems. Stochastic geometry was utilized to model the locations of legitimate and illegitimate receivers and the analytical expressions for the exact and asymptotic secrecy outage probability (SOP) for both single-antenna and multi-antenna scenarios were derived. In [20], the authors investigated the

optimal decoding order, transmission rates, and power allocation in the design of NOMA systems. Two optimization problems were proposed and solved: the transmission power was minimized subject to the secrecy outage and QoS constraints and the minimum secrecy rate was maximized subject to the secrecy outage and transmit power constraints, respectively. Their results indicated that the optimal decoding order would not vary with the secrecy outage constraint in the considered problems and the power allocation ratio to the user must be increased as the secrecy constraint becomes more stringent. In [21], Lv *et al.* proposed a new NOMA-inspired jamming and forwarding scheme to improve the security of cooperative communication systems and derived the analytical expressions for the lower bound of the ergodic secrecy sum rate (ESSR) and the asymptotic ESSR. Three relay selection schemes were proposed to enhance the secrecy performance of the multi-relay cooperative NOMA systems and the analytical expressions for the exact and asymptotic SOP were derived in [22]. In [23], the authors proposed a novel downlink multi-user transmission scheme to meet the heterogeneous service requirements for the airborne NOMA systems consisting of security-sensitive users and QoS-sensitive users. The scenario where the QoS-sensitive users act as potential internal eavesdroppers were considered. The achievable secrecy rate was maximized through the joint optimization of user scheduling, power allocation, and trajectory design. In [24], two new schemes were proposed to enhance the security of airborne NOMA systems by the single user requiring and multiple users requiring security, respectively, and the effectiveness of the proposed schemes in ensuring secure transmissions were analyzed. In [25], the relationship between the reliability and security of a two-user NOMA system was investigated. Considering different decoding capabilities at eavesdroppers and imperfect SIC, the analytical expressions of the SOP under the reliability outage probability constraint were derived. In [26], the authors investigated the secrecy performance of a NOMA-based MEC system using the hybrid SIC decoding scheme. The latency was minimized by jointly optimizing the power allocation, task allocation, and computational resource allocation. A reinforcement learning-based and a matching-based algorithm were proposed to solve the optimization problems for the single-user and multi-user scenarios.

B. Motivation and Contributions

Based on the authors' knowledge, there are two main differences between traditional NOMA and SGF schemes: 1) In traditional NOMA systems, all the NOMA users can utilize the resource blocks, such as time slots or subcarriers. In NOMA-based SGF systems, only the

selected GF users based on scheduling schemes are allowed to opportunistically gain access to those resource blocks that GB users would exclusively occupy. 2) For the conventional NOMA systems, the static SIC technology, either channel state information (CSI)-based SIC or QoS-based SIC, is utilized to cancel inter-user interference. The method in SGF systems to enhance spectral efficiency is through the hybrid (dynamic) SIC scheme. For these reasons, although the secrecy performance of NOMA systems has been investigated in many works, the results are not applicable to NOMA-based SGF systems. This is the motivation for this work. Technically speaking, it is much more challenging to investigate the secrecy performance with a hybrid (dynamic) SIC scheme than that with a static SIC scheme.

We investigate a NOMA-aided SGF system with a single GF user, and then the results have been extended to SGF systems with multiple GF users. The main contributions of this paper are summarized as follows.

1) We analyze the secrecy performance of an uplink NOMA-aided SGF system with a single GF user as a benchmark. The analytical expression for the exact SOP of the GF user is derived. To obtain more insights, we derive asymptotic expressions for the SOP of the GF user in the high transmit signal-to-noise ratio (SNR) regime.

2) We further investigate the secrecy performance of NOMA-aided SGF systems with multiple GF users. The analytical expression for the exact and asymptotic SOP with the BUS scheme is developed based on order statistics to facilitate the performance analysis. Monte Carlo simulation results are provided and compared with two different scheduling schemes. The effects of system parameters on the SOP of the considered system are demonstrated and the accuracy of the developed analytical results is verified.

3) In contrast to the metrics, such as OP and ergodic rate, derived in [12]-[18], the secrecy performance of SGF systems is investigated in this work. Note that it is much more challenging to obtain the analytical expressions of the SOP relative to that of the OP for SGF systems, especially in the presence of multiple GF users.

C. Organization

The rest of this paper is organized as follows. Section II describes the considered system model. The SOP of the SGF systems with a single GF user and multiple GF users are analyzed in Sections III and IV, respectively. Section V presents the numerical and simulation results to

TABLE I: *List of Notations*

Notation	Description
K	Number of the GF users
N	The number of antenna on E
$g_B(g_F)$	Channel coefficient between $U_B(U_F)$ and S
g_k	Channel coefficient between k-th U_F and S
$|H_E|^2$	Channel gains between U_k and E
g_{k_i}	Channel coefficient between k-th GF user and i-th receive antenna at E
$r_F(r_B)$	The distance from U_k (U_B) to S
r_E	The distance from U_k to E
α	Path loss exponent
R_B	Target rate of U_B
R_{th}	Secrecy target rate of U_F
σ^2	The noise power
$P_B(P_F)$	Transmit power of $U_B(U_F)$
$\rho_B(\rho_F)$	Transmit SNR of $U_B(U_F)$
$f_X(\cdot)$	Probability density function of X
$F_X(\cdot)$	Cumulative distribution function of X

demonstrate the analysis and the paper is concluded in Section VI. The notations utilized in this paper are summarized in Table I, which is shown at the top of this page.

II. SYSTEM MODEL

A. NOMA-aided Semi-GF Systems

Consider an uplink SGF system illustrated in Fig. 1, a GB user (U_B) transmits signals to the BS (S), and the channel is re-used by K GF user ($U_k, k = 1, \cdots, K$) in SGF mode. In other words, U_k is allowed to utilize the resource block that would be solely occupied by U_B employing NOMA technology while U_B's QoS experience is the same as when it occupies the channel alone. All the GF users are assumed to transmit signals with the same power ρ_F and the channel gains are ordered as $|h_1|^2 \leq \cdots \leq |h_K|^2$, where $|h_1|^2 = \min_{1 \leq k \leq K} \left(\frac{|g_k|^2}{r_k^\alpha} \right)$ and $|h_K|^2 = \max_{1 \leq k \leq K} \left(\frac{|g_k|^2}{r_k^\alpha} \right)$ where g_k denotes U_k's channel coefficient, r_k denotes the distance between U_k and S, and α signifies the path loss exponent. All the channels are assumed to undergo an independent identically and quasi-static Rayleigh fading model. To facilitate performance analysis, it is
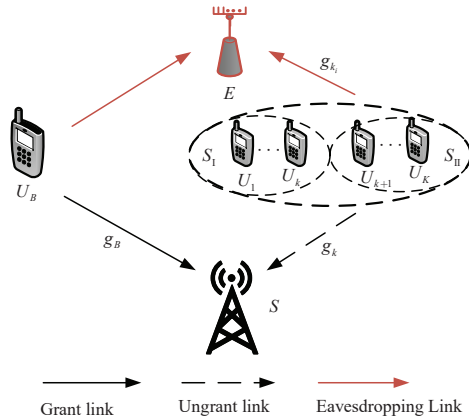
Fig. 1: System model consisting of a BS (S), a GB user (U_B), K GF users (U_k), and an eavesdropper (E) with N antennas. The other nodes are equipped with single antenna.

assumed that all the GF users are located in a small size cluster, such that the distances between U_k and S are same ($r_k = r_F$).

The received signal at S is expressed as $y_B = \sqrt{P_B}h_B x_B + \sqrt{P_F}h_k x_F + n$, where P_i ($i \in \{B, F\}$) denotes the transmit power, $|h_B|^2 = \frac{|g_B|^2}{r_B^\alpha}$, g_B denotes U_B's channel coefficient, r_B denotes the distance between U_B and S, x_i is the signals from U_i with unit power, i.e., $\mathbb{E}\left[|x_i|^2\right] = 1$, and n is the additive white Gaussian noise (AWGN) with zero mean and variance σ^2.

In this work, the BUS scheme is considered, which means the GF user achieving the maximum data rate is scheduled to transmit signals [16], [18]. The admission procedure consists of the following steps [18]: 1) The S sends pilot signals, 2) Each user estimates its own channel state information (CSI), 3) U_B feedbacks its transmit SNR, target rate, and CSI to S, 4) The S calculates U_B's decoding threshold and broadcasts U_B's effective received SNR and decoding threshold to all GF users, 5) Each GF user calculates its transmit data rate, and 6) Each GF user sets its back-off time, which is a strictly decreasing function of the user's data rate. Then the GF user with the maximal data rate will be admitted to transmitting through distributed contention control protocol [12].

To ensure the U_B's QoS, there must have $\log_2\left(1 + \frac{\rho_B |h_B|^2}{1 + \tau\left(|h_B|^2\right)}\right) \geq R_B$, where $\rho_B = \frac{P_B}{\sigma^2}$, R_B denotes the target data of U_B and $\tau\left(|h_B|^2\right) = \max\{0, \tau_B\}$ denotes the maximum interference

power tolerated when U_B's signal is decoded during the first stage of SIC [16] [1], $\tau_B = \frac{|h_B|^2}{\alpha_B} - 1$, $\alpha_B = \frac{\varepsilon_B}{\rho_B}$, $\varepsilon_B = \theta_B - 1$, and $\theta_B = 2^{R_B}$.

S first broadcasts $\tau\left(|h_B|^2\right)$ before scheduling. By comparing their received power of GF's signals on S to $\tau\left(|h_B|^2\right)$, all the GF users are divided into two groups ($\mathcal{S}_{\text{I}}$ and $\mathcal{S}_{\text{II}}$).

- For $U_k \in \mathcal{S}_{\text{I}}$ $(1 \leq k \leq |\mathcal{S}_{\text{I}}| \leq K)$, they experience $\rho_F |h_k|^2 > \tau\left(|h_B|^2\right)$ with $\rho_F = \frac{P_F}{\sigma^2}$, which will lead to $\log_2\left(1 + \frac{\rho_B |h_B|^2}{1 + \tau\left(|h_B|^2\right)}\right) < R_B$. This signifies that U_k's signals must be decoded before decoding U_B's signals to guarantee that U_B's QoS experience is the same as when it occupies the channel alone [2]. Then, the achievable rate of U_B and U_k are expressed as $R_B^{\text{I}} = \log_2\left(1 + \rho_B |h_B|^2\right)$ and $R_k^{\text{I}} = \log_2\left(1 + \frac{\rho_F |h_k|^2}{1 + \rho_B |h_B|^2}\right)$, respectively.

- For those GF users in $U_k \in \mathcal{S}_{\text{II}}$ $(1 \leq k \leq |\mathcal{S}_{\text{II}}| \leq K)$, they experience $\rho_F |h_k|^2 < \tau\left(|h_B|^2\right)$, which will lead to $\log_2\left(1 + \frac{\rho_B |h_B|^2}{1 + \tau\left(|h_B|^2\right)}\right) > R_B$. This signifies that the GF user's signal in this group will be decoded at either the first or the second stage of SIC. Accordingly, U_k will achieve a data of $R_k^{\text{I}} = \log_2\left(1 + \frac{\rho_F |h_k|^2}{1 + \rho_B |h_B|^2}\right)$ or $R_k^{\text{II}} = \log_2\left(1 + \rho_F |h_k|^2\right)$. Due to $R_k^{\text{II}} > R_k^{\text{I}}$, to achieve the maximum data rate at the GF user, U_B's signal must be decoded during the first stage of SIC [16], [18]. Thus, the achievable rate of U_B and U_k are expressed as $R_B^{\text{II}} = \log_2\left(1 + \frac{\rho_B |h_B|^2}{1 + \rho_F |h_k|^2}\right)$ and $R_k^{\text{II}} = \log_2\left(1 + \rho_F |h_k|^2\right)$, respectively.

Then, the achievable rate of U_k $(1 \leq k \leq K - 1)$ is expressed as

$$
R_k = \begin{cases} R_K^{\text{I}}, & |\mathcal{S}_{\text{II}}| = 0, \\ R_K^{\text{II}}, & |\mathcal{S}_{\text{II}}| = K, \\ \max\left\{R_K^{\text{I}}, R_k^{\text{II}}\right\}, & |\mathcal{S}_{\text{II}}| = k. \end{cases}
\tag{1}
$$

It must be noted that only one GF user is selected to access the channel. The grouping stated before is logically grouped for analysis of the achievable rate of the selected GF user. Specifically, the signals from the users in different groups have different decode orders at the base station.

---

[1] The availability of perfect CSI is crucial in deciding the decoding order and the implementation of hybrid SIC. The imperfect power gain caused by imperfect CSI could lead to an inappropriate SIC decoding order being selected and SIC decoding failures occurring [27].

[2] Since the signals from GF users were decoded before decoding those from the GB user in this case, additional latency for GB users will occur. Thus, the GF scheme in the NOMA-aided SGF systems are suitable for such applications with more stringent QoS than latency requirements. In other words, the NOMA-aided SGF systems aim to make a channel reserved by a GB user that can be shared by GF users, improving connectivity and spectral efficiency through collaboration between GF transmission and conventional GB schemes.

Remark 1. *It must be noted the SGF scheme only guarantees that admitting the GF user is transparent to the GB user whose QoS experience is the same as when it occupies the channel alone. In other words, the SGF scheme does not always guarantee no outage for the GB user. Further, the outage of the GB user in this case $\left(|h_B|^2 < \alpha_B\right)$ does not signify outage of the GF user.*

Remark 2. *$\tau\left(|h_B|^2\right) = \max\{0, \tau_B\}$ denotes the maximum interference power tolerated when U_B's signal is decoded during the first stage of SIC. Based on the definition of τ_B, it can be observed that α_B is the threshold when U_B occupies the channel alone. Specifically, due to $\tau_B = \frac{|h_B|^2}{\alpha_B} - 1 < 0 \Leftrightarrow |h_B|^2 < \alpha_B$, α_B signifies the reliability threshold when U_B occupies the channel alone. $|h_B|^2 < \alpha_B$ denotes reliability outage occurs on U_B due to the weakness of the GB link and $\tau_B > 0 \Leftrightarrow |h_B|^2 > \alpha_B$ denotes the channels can be shared with U_F under SGF scheme.*

In this work, we consider the worst-case security scenario wherein E is equipped with N antennas using maximal ratio combining (MRC) scheme to fully decode the users' information [3]. Then, the eavesdropping rate is expressed as $R_E = \log_2\left(1 + \rho_F |H_E|^2\right)$, where $|H_E|^2 \triangleq \sum_{i=1}^{N} |h_{k_i}|^2$, $|h_{k_i}|^2 = \frac{|g_{k_i}|^2}{r_E^\alpha}$, $|g_{k_i}|^2$ denotes channel coefficient between k-th GF user and i-th receive antenna at E, and r_E denotes the distance between the GF users and E.

B. Statistical Properties of Channel Power Gains

This subsection provides the statistical law of channel power gains, laying the performance analysis foundation. The probability density function (PDF) of $|H_E|^2$ is expressed as $f_{H_E}(x) = \frac{r_E^{N\alpha}}{\Gamma(N)} x^{N-1} e^{-r_E^{N\alpha} x}$, where $\Gamma(z) = \int_0^\infty e^{-t} t^{z-1} dt$ is the Gamma function as defined by [30, (8.310.1)]. The CDF of $|h_K|^2$ is expressed as $F_{|h_K|^2}(x) = \sum_{i=0}^{K} \varphi_i e^{-ir_F^\alpha x}$, where $\varphi_i = \binom{K}{i}(-1)^i$, and $\binom{K}{i} = \frac{K!}{i!(K-i)!}$.

---

[3]In this case, it is assumed that the eavesdropper has a powerful multi-user detection capability (e.g. parallel interference cancellation) so that the received data stream can be distinguished and the interference generated by the superimposed signals can be subtracted [37]. As stated in [19], [25], this case is the worst-case scenario where the decoding capability of the eavesdropper has been overestimated, which makes the analysis and design robust for the practical scenario and is sensible and desirable from a security perspective.

The joint PDF of $|h_i|^2$ and $|h_j|^2 (1 \leqslant i < j \leqslant K)$ is expressed as [16]

$$f_{|h_i|^2,|h_j|^2}(x,y) = \sum_{n=0}^{j-i-1} \sum_{m=0}^{i-1} \phi_1 e^{-\phi_2 x - \phi_3 y}, \tag{2}$$

where $\phi_1 = \frac{K!(-1)^{m+n}\binom{j-i-1}{n}\binom{i-1}{m}r_F^{2\alpha}}{(i-1)!(K-j)!(j-i-1)!}$, $\phi_2 = r_F^\alpha(m+j-i-n)$, and $\phi_3 = r_F^\alpha(K-j+n+1)$.

Then, the joint CDF of $|h_i|^2$ and $|h_j|^2$ $(1 \leqslant i < j \leqslant K)$ is obtained as

$$F_{|h_i|^2,|h_j|^2}(x,y) = \sum_{n=0}^{j-i-1} \sum_{m=0}^{i-1} \frac{\phi_1}{\phi_3} \left(\frac{e^{-(\phi_2+\phi_3)x}}{\phi_2+\phi_3} + \frac{\phi_3 e^{-(\phi_2+\phi_3)y}}{\phi_2(\phi_2+\phi_3)} - \frac{e^{-\phi_2 x - \phi_3 y}}{\phi_2} \right). \tag{3}$$

When $i=1, j=K$, we obtain

$$f_{|h_1|^2,|h_K|^2}(x,y) = \sum_{n=0}^{K-2} \mu_0 e^{-r_F^\alpha(K-n-1)x} e^{-r_F^\alpha(n+1)y}, \tag{4}$$

and

$$F_{|h_1|^2,|h_K|^2}(x,y) = \sum_{n=0}^{K-2} \mu_1 e^{-Kr_F^\alpha x} + \mu_2 e^{-Kr_F^\alpha y} - \mu_3 e^{-(K-n-1)r_F^\alpha x} e^{-(n+1)r_F^\alpha y}, \tag{5}$$

respectively, where $\mu_0 = \frac{K!(-1)^n\binom{K-2}{n}r_F^{2\alpha}}{(K-2)!}$, $\mu_1 = \frac{\mu_0}{r_F^{2\alpha}K(n+1)}$, $\mu_2 = \frac{\mu_0}{r_F^{2\alpha}K(K-n-1)}$, $\mu_3 = \frac{\mu_0}{r_F^{2\alpha}(n+1)(K-n-1)}$.

The joint PDF and CDF of $|h_k|^2$, $|h_{k+1}|^2$ $(1 \leq k \leq K-2)$, and $|h_K|^2$ is given as [16]

$$f_{|h_k|^2,|h_{k+1}|^2,|h_K|^2}(x,y,z) = \sum_{n=0}^{K-k-2} \sum_{m=0}^{k-1} \varsigma_0 e^{-A_0 x} e^{-B_0 y} e^{-C_0 z}, \tag{6}$$

and

$$F_{|h_k|^2,|h_{k+1}|^2,|h_K|^2}(x,y,z,w) = \sum_{n=0}^{K-k-2} \sum_{m=0}^{k-1} \sum_{i=1}^{6} \varsigma_i e^{-(A_i x + B_i y + C_i z + W_i w)}, \tag{7}$$

respectively, where $\varsigma_0 = \frac{K!(-1)^{m+n}\binom{K-k-2}{n}\binom{k-1}{m}r_F^{3\alpha}}{(K-k-2)!(k-1)!}$, $A_0 = r_F^\alpha(m+1)$, $B_0 = r_F^\alpha(K-k-n-1)$, $C_0 = r_F^\alpha(n+1)$, $W_0 = B_0 + C_0$, $\varsigma_1 = -\varsigma_2 = \frac{\varsigma_0}{A_0 B_0 C_0}$, $\varsigma_3 = -\varsigma_4 = -\frac{\varsigma_0}{A_0 B_0 W_0}$, $\varsigma_5 = -\varsigma_6 = -\frac{\varsigma_0}{A_0 C_0 W_0}$, $A_1 = A_3 = A_5 = 0$, $A_2 = A_4 = A_6 = A_0$, $B_1 = B_3 = B_5 = A_0$, $B_2 = B_4 = B_6 = 0$, $C_1 = C_2 = B_0$, $C_3 = C_4 = 0$, $C_5 = C_6 = W_0$, $W_1 = W_2 = C_0$, $W_3 = W_4 = W_0$, and $W_5 = W_6 = 0$.

For $k = K-1$, we have $|h_{k+1}|^2 = |h_K|^2$, the joint PDF and CDF of $|h_{K-1}|^2$ and $|h_K|^2$ are expressed as

$$f_{|h_{K-1}|^2,|h_K|^2}(x,y) = \sum_{n=0}^{K-2} \mu_0 e^{-C_0 x} e^{-r_F^\alpha y}, \tag{8}$$

and

$$F_{|h_{K-1}|^2,|h_K|^2}(x,y,z,w) = \sum_{n=0}^{k-2} \sum_{j=1}^{4} \frac{\mu_0}{C_0} (-1)^{j+1} e^{-(a_j x + b_j y + c_j z + q_j w)}, \tag{9}$$

respectively, where $a_1 = a_4 = 0, a_2 = a_3 = C_0, b_1 = b_4 = C_0, b_2 = b_3 = 0, c_1 = c_2 = 0,$ $c_3 = c_4 = r_F^\alpha$, $q_1 = q_2 = r_F^\alpha$, and $q_3 = q_4 = 0$.

III. SECRECY OUTAGE PROBABILITY ANALYSIS WITH A SINGLE GRANT-FREE USER

In this section, the secrecy performance of the SGF systems with a single GF user is investigated to pay the road to the performance analysis of SGF systems with multiple GF users. When $K = 1$, there is no need to consider scheduling. It must be noted that this scenario can also be viewed as the multiple-GF-user SGF systems using a random user scheduling (RUS) scheme. The achievable rate of U_F in (1) is rewritten as

$$R_F = \begin{cases} R_F^{\mathrm{I}}, & \rho_F |h_F|^2 > \tau \left(|h_B|^2 \right), \\ R_F^{\mathrm{II}}, & \rho_F |h_F|^2 < \tau \left(|h_B|^2 \right), \end{cases} \tag{10}$$

where $R_F^{\mathrm{I}} = \log_2 \left(1 + \frac{\rho_F |h_F|^2}{1 + \rho_B |h_B|^2} \right)$ and $R_F^{\mathrm{II}} = \log_2 \left(1 + \rho_F |h_F|^2 \right)$, which denote the achievable rate at U_F in scenarios when U_F's signal is decoded at the first and second stages of the SIC, respectively. It must be noted that when there is an outage on U_B, the U_F' signals must be decoded at the first stage of the SIC.

The user U_j's achievable secrecy rate is expressed as $R_{s,j}^i = \left[R_j^i - R_E \right]^+$[28], where $j \in \{F, B\}$, $i \in \{\mathrm{I}, \mathrm{II}\}$ and $[x]^+ = \max \{x, 0\}$. SOP denotes the probability that the maximum achievable secrecy rate is less than a target secrecy rate [28]. Based on (10), the SOP for U_F is given as

$$P_{out,F} = \underbrace{\Pr \left\{ R_{s,F}^{\mathrm{I}} < R_{th}, \rho_F |h_F|^2 > \tau \left(|h_B|^2 \right) \right\}}_{P_{out}^{\mathrm{I}}} + \underbrace{\Pr \left\{ R_{s,F}^{\mathrm{II}} < R_{th}, \rho_F |h_F|^2 < \tau \left(|h_B|^2 \right) \right\}}_{P_{out}^{\mathrm{II}}},$$
$$\tag{11}$$

where R_{th} represents the secrecy threshold rate, P_{out}^{I} denotes U_F's signal is decoded at the first stage, and P_{out}^{II} denotes U_F's signal is decoded at the second stage.

Similarly, the SOP for U_B is expressed as

$$P_{out,B} = \Pr \left\{ R_{s,B}^{\mathrm{I}} < R_{th}, \rho_F |h_F|^2 > \tau \left(|h_B|^2 \right) \right\} + \Pr \left\{ R_{s,B}^{\mathrm{II}} < R_{th}, \rho_F |h_F|^2 < \tau \left(|h_B|^2 \right) \right\}. \tag{12}$$

It can be observed that the analysis of the secrecy outage probability of the GB user is similar to that of the GF user, expressed in Eq. (11). Due to space limitations, the analysis of the U_B's secrecy outage probability is regrettably omitted here. In this work, the SOP of the NOMA-aided SGF system is equivalent to the SOP of the GF user, unless stated otherwise.

Remark 3. *It must be noted that ρ_B affects the SNR/SINR of U_B and the maximum interference that U_B can tolerate when U_B's signal is decoded during the first stage of SIC simultaneously. In the lower-ρ_B region, the signals from U_F must be decoded in the first stage of SIC. With the increase of ρ_B, the interference to U_F increases and the secrecy performance worsens. In the larger-ρ_B region, the signals from U_F will be decoded in the second stage of SIC. There is no interference from U_B to U_F. Then, the SOP decreases to a constant. Thus, there is a worst ρ_B for the security of U_F.*

Remark 4. *In contrast, ρ_F affects the SNR/SINR of U_F and E simultaneously. In the lower-ρ_F region, the signals from U_B will be decoded in the first stage of SIC. For a small ρ_F, there is $\Pr\left\{\rho_F|h_F|^2 < \tau\left(|h_B|^2\right)\right\} > \Pr\left\{\rho_F|h_F|^2 > \tau\left(|h_B|^2\right)\right\}$. Thus, P_{out}^{II} is the main part of P_{out} in the lower-ρ_F region while P_{out}^{I} is the main part of P_{out} in the larger-ρ_F region. Based on the results in [29], increasing ρ_F will enhance the security of U_F in the lower-ρ_F region. In the larger-ρ_F region, the signals from U_F will be decoded in the first stage of SIC. Although both the SINR of U_F and SNR of E improve with increasing ρ_F, the SINR of U_F improves slower than the SNR of E, so the security of the SGF system deteriorates. Thus, there is an optimal ρ_F to minimize the SOP of U_F.*

Remark 5. *Furthermore, the effect from r_B on $P_{out}^{\mathrm{I}}\left(P_{out}^{\mathrm{II}}\right)$ is the opposite of the effect from ρ_B, while the effect of ρ_B and r_B on the secrecy performance of the SGF systems are similar. r_F only affects the SINR/SNR of U_F. Larger r_F denotes stronger path loss on U_F thereby higher SOP. r_E only affects the SNR of E where larger r_E denotes stronger path loss on E and hence lower SOP.*

The following theorem provides an exact expression for the SOP achieved applicable to the considered SGF scheme.

Theorem 1. *The SOP of U_F is expressed as*

$$P_{out} = \begin{cases} P_{out}^{\mathrm{I},1} + P_{out}^{\mathrm{I},21} + P_{out}^{\mathrm{II}}, & \varepsilon_B\varepsilon_{th} < 1, \\ P_{out}^{\mathrm{I},1} + P_{out}^{\mathrm{I},22} + P_{out}^{\mathrm{II}}, & \varepsilon_B\varepsilon_{th} > 1, \end{cases} \tag{13}$$

where $P_{out}^{\mathrm{I},1} = 1 - e^{-r_B^\alpha \alpha_B} - \frac{r_B^\alpha r_E^{N\alpha} e^{-r_F^\alpha \alpha_{th}} \omega_1(\lambda_1,\lambda_2,\lambda_3)}{\Gamma(N)}$, $P_{out}^{\mathrm{I},21} = \frac{e^{-r_B^\alpha \alpha_B} r_B^\alpha \Gamma(N, r_E^\alpha \alpha_1)}{\varepsilon_2 \Gamma(N)} + e^{\frac{r_F^\alpha}{P_F}} r_B^\alpha r_E^{N\alpha} \frac{\omega_3\left(0,\varepsilon_2,r_E^\alpha\right)}{\Gamma(N)}$ $-e^{-r_F^\alpha \alpha_{th}} r_B^\alpha r_E^{N\alpha} \frac{\omega_2(\lambda_1,\lambda_2,\lambda_3)+\omega_3(\lambda_1,\lambda_2,\lambda_3)}{\Gamma(N)}$, $P_{out}^{\mathrm{I},22} = r_B^\alpha \frac{e^{-r_B^\alpha \alpha_B}}{\varepsilon_2} - r_B^\alpha r_E^{N\alpha} \frac{e^{-r_F^\alpha \alpha_{th}} \omega_4(\lambda_1,\lambda_2,\lambda_3)}{\Gamma(N)}$, $P_{out}^{\mathrm{II}} = \frac{r_F^\alpha e^{-r_B^\alpha \alpha_B}}{r_B^\alpha P_F \alpha_B + r_F^\alpha}$ $-\frac{r_E^{N\alpha} r_F^\alpha e^{-(r_F^\alpha \alpha_{th}+r_B^\alpha \varepsilon_1)}}{\left(r_F^\alpha \rho_F \alpha_B + r_B^\alpha\right)\left(r_B^\alpha \rho_F \varepsilon_1 + \lambda_3\right)^N}$, $\alpha_{th} = \frac{\varepsilon_{th}}{\rho_F}$, $\varepsilon_{th} = \theta_{th} - 1$, $\theta_{th} = 2^{R_{th}}$, $\lambda_1 = r_F^\alpha \rho_B \theta_{th}$, $\lambda_2 =$

$r_F^\alpha \rho_B \alpha_{th} + r_B^\alpha$, $\lambda_3 = r_F^\alpha \theta_{th} + r_E^\alpha$, $\alpha_1 = \frac{1 - \varepsilon_B \varepsilon_{th}}{\rho_F \theta_{th} \varepsilon_B}$, $\varepsilon_1 = \alpha_B \theta_{th}$, $\varepsilon_2 = \frac{r_F^\alpha}{P_F \alpha_B} + r_B^\alpha$, $\Gamma(\cdot, \cdot)$ is the upper incomplete Gamma function, as defined by [30, (8.350.2)], $\omega_1(a,b,c) = \frac{b^{N-1}\Gamma(N)}{a^N} e^{\frac{bc}{a}}$
$\times \left(\Gamma\left(1 - N, \frac{bc}{a}\right) - \Gamma\left(1 - N, b\alpha_B + \frac{bc}{a}\right) \right)$, $\omega_2(a,b,c) = \frac{b^{N-1}\Gamma(N)}{a^N} e^{\frac{bc}{a}} \Gamma\left(1 - N, b\alpha_B + \frac{bc}{a}\right) - e^{-b\alpha_B}\Delta$,
$\Delta = \frac{\pi \alpha_1}{2R} \sum_{r=1}^{R} \frac{\sqrt{1 - \ell_r^2}}{a\hbar_r + b} \hbar_r^{N-1} e^{-(a\alpha_B + c)\hbar_r}$, $\omega_3(a,b,c) = \frac{b^{N-1}\Gamma(N)}{a^N} e^{\frac{bc}{a}} \Gamma\left(1 - N, b\alpha_B + \frac{bc}{a}\right) - \omega_2(a,b,c) -$
$e^{\frac{b}{P_B} - a\alpha_3} \frac{\pi \alpha_1}{2L} \sum_{l=1}^{L} \frac{\sqrt{1 - \vartheta_l^2}}{av_l + b} v_l^{N-1} \times e^{\left(\frac{a}{P_B} - c\right)v_l - \frac{\alpha_3(a\alpha_1 + b)}{\alpha_1 - v_l}}$, $\omega_4(a,b,c) = \frac{b^{N-1}\Gamma(N)}{a^N} e^{\frac{bc}{a}} \Gamma\left(1 - N, b\alpha_B + \frac{bc}{a}\right)$,
R and L is the summation item, which reflects accuracy vs. complexity, $\ell_r = \cos\left(\frac{2r-1}{2R}\pi\right)$, $\hbar_r = \frac{\alpha_1}{2}(\ell_r + 1)$, $\vartheta_l = \cos\left(\frac{2l-1}{2L}\pi\right)$, and $v_l = \frac{\alpha_1}{2}(\vartheta_l + 1)$.

Proof. See Appendix A. □

Remark 6. *Based on (A.1), one can observe that $\Pr\{\rho_F|h_F|^2 > 0\} = 1$, which is independent of ρ_F. With the help of the result in [29], secrecy capacity improves with increasing transmit SNR then gradually tends to a constant. So, $P_{out}^{I,1}$ decreases and gradually tends to a constant for a given α_B. Furthermore, $\Pr\left\{|h_F|^2 > \frac{\tau_B}{\rho_F}\right\}$ increases gradually tending to 1 with increasing ρ_F. Thus, for a given α_B, $P_{out}^{I,2}$ increases with increasing ρ_F until gradually tending to a constant and independent of ρ_F.*

Remark 7. *Based on (A.3), it must be noted that the relationship between $\omega_0\left(|h_B|^2, |H_E|^2\right)$ and $\frac{\tau_B}{\rho_F}$ act as the constraint for the GF link. More specifically, the former is constraint on security while the latter is constraint on decoding order. The relationship between constraint on security and on decoding order directly affects the SOP of U_F.*

Remark 8. *The analysis in (A.4) demonstrates that SOP of U_F depends on the relationship between $\varepsilon_B \varepsilon_{th}$ and 1, which determines the relationship between the constraint on decoding order and the constraint on security. When $\varepsilon_B \varepsilon_{th} > 1$, the constraint on decoding order is always less than that on security. $\epsilon_B \epsilon_{th} < 1$ means that R_{th} needs to be small for a given R_B, which is a generalized condition in practice since SGF is invoked to encourage spectrum sharing between a GB user and a GF user with a low secrecy threshold data rate. However, for $\epsilon_B \epsilon_{th} > 1$, it also offers secrecy outage performance achieved by the SGF scheme will be worse.*

The analytical expression provided in (13) is complicated because many factors affect the secrecy performance of the GF user, specifically, the decoding order, the target data rate of U_B, the target secrecy rate of U_F, and the quality of the eavesdropping channel. We derive asymptotic expressions of the SOP in the high transmit SNR regime to obtain more insights.

Corollary 1. *When $\rho_B \to \infty$, the asymptotic SOP of U_F is approximated as*

$$P_{out}^{\rho_B \to \infty} \approx P_{out}^{\text{II},\rho_B \to \infty} = 1 - e^{-r_F^\alpha \alpha_{th}} \left(1 + \left(\frac{r_F}{r_E}\right)^\alpha \theta_{th}\right)^{-N}. \tag{14}$$

Proof. See Appendix B. □

Remark 9. *The increasing ρ_B leads to larger $\tau\left(|h_B|^2\right)$, which means it is easy to guarantee the QoS of U_B. Then, the probability of decoding the U_F's signals in the second stage of SIC increases. The final result is $P_{out} \approx \Pr\left\{R_s^{\text{II}} < R_{th}\right\}$ which simply depends on ρ_F, R_{th}, r_F, r_E, and N.*

Corollary 2. *When $\rho_F \to \infty$, the asymptotic SOP of U_F is approximated as*

$$P_{out}^{\rho_F \to \infty} \approx P_{out}^{\text{I},\rho_F \to \infty} = 1 - \left(\frac{r_B}{r_F}\right)^{N\alpha} \left(\frac{r_E^\alpha}{\rho_B \theta_{th}}\right)^N \Gamma\left(1 - N, \frac{r_B^\alpha}{\rho_B \theta_{th}}\left(\theta_{th} + \left(\frac{r_E}{r_F}\right)^\alpha\right)\right). \tag{15}$$

Proof. See Appendix C. □

Remark 10. *The increasing ρ_F leads to $\Pr\left\{\rho_F |h_F|^2 < \tau\left(|h_B|^2\right)\right\} \to 0$, which leads to $P_{out}^{\text{II}} \to 0$. Then, the probability of decoding the U_F's signals in the first stage of SIC increases. The final result is $P_{out} \approx \Pr\left\{R_s^{\text{I}} < R_{th}\right\}$, which depends on ρ_B, R_{th}, r_B, r_E, and N.*

Corollary 3. *When $\rho_B = \rho_F \to \infty$, the asymptotic SOP of U_F is approximated as*

$$P_{out}^\infty = P_{out}^{\text{I},\infty} + P_{out}^{\text{II},\infty} = 1 - \left(1 + \left(\frac{r_B}{r_F}\right)^\alpha \varepsilon_B\right)^{-1} \left(1 + \theta_{th}\left(\frac{r_F}{r_E}\right)^\alpha + \varepsilon_B \theta_{th}\left(\frac{r_B}{r_E}\right)^\alpha\right)^{-N}. \tag{16}$$

Proof. See Appendix D. □

Remark 11. *In this scenarios with $\rho_B = \rho_F \to \infty$, it must be noted that there is $\Pr\left\{\rho_F |h_F|^2 < \tau\left(|h_B|^2\right)\right\} = \Pr\left\{|h_F|^2 < \frac{|h_B|^2}{\varepsilon_B}\right\}$. The decoding order depends on the relationship between $\frac{|g_F|^2}{r_F^\alpha}$ and $\frac{|h_B|^2}{\varepsilon_B} = \frac{|g_B|^2}{r_B^\alpha(2^{R_B}-1)}$. Then, we have $P_{out}^{\text{I}} = \Pr\left\{R_s^{\text{I}} < R_{th}, |h_F|^2 > \frac{|h_B|^2}{\varepsilon_B}\right\}$ and $P_{out}^{\text{II}} = \Pr\left\{R_s^{\text{II}} < R_{th}, |h_F|^2 < \frac{|h_B|^2}{\varepsilon_B}\right\}$, which are constants independent of ρ_B and ρ_F depends on R_B, R_{th}, r_B, r_F, and r_E.*

IV. SECRECY OUTAGE PROBABILITY ANALYSIS WITH MULTIPLE GRANT-FREE USERS

In this section, the secrecy performance of the multiple-GF-user SGF systems with BUS scheme is investigated.

A. Secrecy Outage Probability Analysis

When $K > 1$, both user scheduling and decoding order issues should be considered simultaneously. It should be noted that $|\mathcal{S}_{\mathrm{II}}| = K$ denotes that the signals from GF users should be decoded on the secondary stage of SIC to maximize the achievable rate. Then U_K is selected to transmit signals. The same for $|\mathcal{S}_{\mathrm{II}}| = 0$. Based on (1), the SOP of U_k is given by

$$P_{out} = \underbrace{\Pr\left\{R_K^{\mathrm{I}} - R_E < R_{th}, |\mathcal{S}_{\mathrm{II}}| = 0\right\}}_{\triangleq P_{out,1}} + \underbrace{\Pr\left\{R_K^{\mathrm{II}} - R_E < R_{th}, |\mathcal{S}_{\mathrm{II}}| = K\right\}}_{\triangleq P_{out,2}}$$
$$+ \underbrace{\sum_{k=1}^{K-1} \Pr\left\{\max\left\{R_K^{\mathrm{I}}, R_k^{\mathrm{II}}\right\} - R_E < R_{th}, |\mathcal{S}_{\mathrm{II}}| = k\right\}}_{\triangleq P_{out,3}}, \tag{17}$$

where $P_{out,1}$ denotes the SOP for U_k when groups $\mathcal{S}_{\mathrm{II}}$ are empty, $P_{out,2}$ signifies the SOP for U_k when groups $\mathcal{S}_{\mathrm{I}}$ are empty, and $P_{out,3}$ denotes the SOP for U_k when there are k GF users in groups $\mathcal{S}_{\mathrm{II}}$. In the first two terms, U_K is always selected to transmit signals. The following theorem provides the exact expression for the SOP of the considered SGF scheme with multiple GF users.

Theorem 2. *The SOP of U_F is expressed as*

$$P_{out} = \begin{cases} P_{out,1}^1 + P_{out,1}^{21} + P_{out,2} + P_{out,3}, & \varepsilon_B \varepsilon_{th} < 1, \\ P_{out,1}^1 + P_{out,1}^{22} + P_{out,2} + P_{out,3}, & \varepsilon_B \varepsilon_{th} > 1, \end{cases} \tag{18}$$

where $P_{out,1}^1 = 1 - e^{-r_B^\alpha \alpha_B} - \dfrac{r_B^\alpha r_E^{N\alpha} e^{-r_F^\alpha \alpha_{th}} \omega_1(\lambda_1,\lambda_2,\lambda_3)}{\Gamma(N)}$, $P_{out,1}^{21} = \dfrac{r_B^\alpha r_E^{N\alpha}}{\Gamma(N)} \sum\limits_{n=0}^{K-2} \sum\limits_{i=2}^{i=3} \left(\mu_1 e^{\frac{Kr_E^\alpha}{\rho_F}} \omega_i\left(0, \alpha_4, r_E^\alpha\right) \right.$

$+ \mu_2 e^{-Kr_F^\alpha \alpha_{th}} \omega_i\left(\eta_1, \eta_2, \eta_3\right) - \mu_3 e^{\frac{Kr_F^\alpha - C_0}{\rho_F} - C_0 \alpha_{th}} \left. \omega_i\left(\eta_4, \eta_5, \eta_6\right) \right)$, $P_{out,1}^{22} = \dfrac{r_B^\alpha r_E^{N\alpha}}{\Gamma(N)} \sum\limits_{n=0}^{K-2} \left(\mu_1 e^{\frac{Kr_E^\alpha}{\rho_F}} \times \right.$

$\omega_4\left(0, \alpha_4, r_E^\alpha\right) + \mu_2 e^{-Kr_F^\alpha \alpha_{th}} \omega_4\left(\eta_1, \eta_2, \eta_3\right) - \mu_3 e^{\frac{Kr_F^\alpha - C_0}{\rho_F} - C_0 \alpha_{th}} \left. \omega_4\left(\eta_4, \eta_5, \eta_6\right) \right)$, $P_{out,2} =$

$\sum\limits_{i=0}^{K} \left(\dfrac{\varphi_i}{ir_F^\alpha + r_B^\alpha \rho_F \alpha_B} \left(\dfrac{ir_F^\alpha r_E^{N\alpha} e^{-(ir_F^\alpha \alpha_{th} + r_B^\alpha \varepsilon_1)}}{\left(ir_F^\alpha \theta_{th} + r_B^\alpha \rho_F \varepsilon_1 + r_E^\alpha\right)^N} + \rho_F \alpha_B r_B^\alpha e^{-r_B^\alpha \alpha_B} \right) \right)$, $P_{out,3} = r_B^\kappa r_E^{N\kappa} \sum\limits_{n=0}^{K-k-2} \sum\limits_{m=0}^{k-1} \left(\sum\limits_{i=1}^{4} \dfrac{\varsigma_i}{\Gamma(N)} \right.$

$\times \left(e^{-\xi_1} \Delta_1 + e^{-\xi_4} \Delta_3\right) + \sum\limits_{i=5}^{6} \varsigma_i \left(e^{-\xi_1} \Delta_2 + e^{-\xi_4} \Delta_4\right) \Big) + r_B^\kappa r_E^{N\kappa} \sum\limits_{n=0}^{K-2} \dfrac{\mu_0}{C_0} \left(\sum\limits_{j=1}^{2} \dfrac{(-1)^{j+1}}{\Gamma(N)} \left(e^{-\zeta_1} \Delta_5 + e^{-\zeta_4} \Delta_7\right) \right.$

$+ \sum\limits_{j=3}^{4} (-1)^{j+1} \left(e^{-\zeta_1} \Delta_6 + e^{-\zeta_4} \Delta_8\right) \Big)$, $\alpha_4 = \dfrac{Kr_F^\alpha}{\rho_F \alpha_B} + r_B^\alpha$, $\eta_1 = Kr_F^\alpha \rho_B \theta_{th}$, $\eta_2 = Kr_F^\alpha \rho_B \alpha_{th} + r_B^\alpha$,

$\eta_3 = Kr_F^\alpha \theta_{th} + r_E^\alpha$, $\eta_4 = C_0 \rho_B \theta_{th}$, $\eta_5 = C_0 \rho_B \alpha_{th} + \dfrac{Kr_F^\alpha - C_0}{\rho_F \alpha_B} + r_B^\alpha$, $\eta_6 = C_0 \theta_{th} + r_E^\alpha$, $\Delta_1 =$

$\dfrac{\xi_3^{N-1} \Gamma\left(1 - N, \xi_3 \alpha_B + \frac{\xi_2 \xi_3}{u_1}\right)}{u_1^N} e^{\frac{\xi_2 \xi_3}{u_1}} - \dfrac{e^{-\xi_3 \varepsilon_1} \omega_5(u_1, \xi_3, v_1, l_1)}{\Gamma(N)}$, $\Delta_2 = \dfrac{e^{-\xi_3 \alpha_B}}{\xi_2^N \xi_3} - \dfrac{e^{-\xi_3 \varepsilon_1}}{\xi_3(\rho_F \xi_3 \varepsilon_1 + \xi_2)^N}$, $\xi_1 = W_i \alpha_{th} - \dfrac{B_i + C_i}{\rho_F}$,

$\xi_2 = W_i \theta_{th} + r_E^\alpha$, $\xi_3 = W_i \rho_B \alpha_{th} + \dfrac{B_i + C_i}{P_F \alpha_B} + r_B^\alpha$, $u_1 = W_i \rho_B \theta_{th}$, $v_1 = u_1 \rho_F \varepsilon_1$, $l_1 = u_1 \varepsilon_1 +$

$\rho_F \xi_3 \varepsilon_1 + \xi_2$, $\xi_4 = (B_i + W_i) \alpha_{th} - \dfrac{C_i}{\rho_F}$, $\omega_5\left(a, b, c, f\right) = \dfrac{f^{N-1}}{b} H_{1,0:1,1:0,1}^{1,0:1,1:1,0} \left[\begin{matrix} (0;1,2) \\ - \end{matrix} \middle| \begin{matrix} (0,1) \\ (0,1) \end{matrix} \middle| \begin{matrix} - \\ (0,1) \end{matrix} \middle| \dfrac{a}{bf}, \dfrac{c}{f^2} \right]$,

$$\Delta_3 = \frac{e^{-\xi_6 \varepsilon_1} \omega_6(u_1, \xi_6, v_2, l_2)}{\Gamma(N)}, \quad \Delta_4 = \frac{e^{-\xi_6 \varepsilon_1}}{\xi_6 (\rho_F \xi_6 \varepsilon_1 + \xi_5)^N}, \quad v_2 = u_1 \rho_F \varepsilon_1, \quad l_2 = u_1 \varepsilon_1 + \xi_6 \rho_F \varepsilon_1 + \xi_5, \quad \xi_5 =$$

$$(B_i + W_i)\theta_{th} + r_E^\alpha, \quad \xi_6 = W_i \alpha_{th} \rho_B + \frac{C_i}{P_F \alpha_B} + r_B^\alpha, \quad \zeta_1 = q_j \alpha_{th} - \frac{b_j + c_j}{\rho_F}, \quad \zeta_2 = q_j \theta_{th} + r_E^\alpha, \quad \zeta_3 =$$

$$q_j \alpha_{th} \rho_B + \frac{b_j + c_j}{P_F \alpha_B} + r_B^\alpha, \quad \Delta_5 = \frac{\zeta_3^{N-1}}{u_2^N} e^{\frac{\zeta_2 \zeta_3}{u_2}} \Gamma\left(1 - N, \zeta_3 \alpha_B + \frac{\zeta_2 \zeta_3}{u_2}\right) - \frac{e^{-\xi_3 \varepsilon_1} \omega_5(u_2, \zeta_3, v_3, l_3)}{\Gamma(N)}, \quad u_2 = q_j \rho_B \theta_{th},$$

$$v_3 = u_2 \rho_F \varepsilon_1, \quad l_3 = u_2 \varepsilon_1 + \zeta_3 \rho_F \varepsilon_1 + \zeta_2, \quad \Delta_6 = \frac{e^{-\zeta_3 \alpha_B}}{\zeta_2^N \zeta_3} - \frac{e^{-\zeta_3 \varepsilon_1}}{\zeta_3 (P_F \zeta_3 \varepsilon_1 + \zeta_2)^N}, \quad \zeta_4 = (b_j + q_j) \alpha_{th} - \frac{c_i}{\rho_F},$$

$$\zeta_5 = (b_j + q_j)\theta_{th} + r_E^\alpha, \quad \zeta_6 = q_i \alpha_{th} \rho_B + \frac{c_j}{P_F \alpha_B} + r_B^\alpha, \quad \Delta_7 = \frac{e^{-\zeta_6 \varepsilon_1} \omega_5(u_2, \zeta_6, v_4, l_4)}{\Gamma(N)}, \quad v_4 = u_2 \rho_F \varepsilon_1,$$

$$l_4 = u_2 \varepsilon_1 + \zeta_6 \rho_F \varepsilon_1 + \zeta_5, \text{ and } \Delta_8 = \frac{e^{-\zeta_6 \varepsilon_1}}{\zeta_6 (\rho_F \zeta_6 \varepsilon_1 + \zeta_5)^N}.$$

Proof. See Appendix E. □

Remark 12. *Based on (E.11), it can be observed that the number of the users in Groups I and II depends on the relationship between $|h_k|^2$ and $\frac{\tau_B}{\rho_F} = \frac{\rho_B}{\rho_F} \frac{|h_B|^2}{2^{R_B}-1} - \frac{1}{\rho_F}$ related to ρ_B and ρ_F.*

Relative to SGF systems with a single GF user, the expression of SOP presented in **Theorem 2** is exceptionally complicated, and the main reason is that in addition to the factors highlighted in **Theorem 1**, the number of users in each group has a significant effect on the secrecy performance.

B. Asymptotic Secrecy Outage Probability Analysis

To obtain more insights, we derive asymptotic expressions of the SOP in the high transmit SNR regime.

Corollary 4 When $\rho_B = \rho_F \to \infty$, the SOP of U_k is approximated at high SNR as

$$P_{out}^\infty \approx P_{out,1}^{2,\infty} + P_{out,2}^\infty + P_{out,3}^\infty, \tag{19}$$

where $P_{out,1}^{2,\infty} \approx \sum_{n=0}^{K-2} \frac{\varepsilon_B \mu_1}{K\left(\frac{r_F}{r_B}\right)^\alpha + \varepsilon_B}$, $P_{out,2}^\infty \approx \sum_{i=0}^{K} \frac{\varphi_i \varepsilon_B}{i\left(\frac{r_F}{r_B}\right)^\alpha + \varepsilon_B} + \sum_{i=0}^{K} \frac{i\varphi_i (i\chi_1 + \chi_2)^{-N}}{i + \varepsilon_B \left(\frac{r_B}{r_F}\right)^\alpha}$, $\chi_1 = \theta_{th}\left(\frac{r_F}{r_E}\right)^\alpha$,

$\chi_2 = \varepsilon_B \theta_{th}\left(\frac{r_B}{r_E}\right)^\alpha + 1$, $P_{out,3}^\infty = \sum_{k=1}^{K-2} P_{out,3}^{k,\infty} + P_{out,3}^{K-1,\infty} = \sum_{k=1}^{K-2}(I_3^\infty + I_4^\infty) + P_{out,3}^{K-1,\infty}$, $I_3^\infty \approx$

$\sum_{n=0}^{K-k-2}\sum_{m=0}^{k-1}\sum_{i=5}^{6} \frac{\varsigma_i \varepsilon_B (1-\chi_3)}{(K+\varpi_i)\left(\frac{r_F}{r_B}\right)^\alpha + \varepsilon_B}$, $I_4^\infty \approx \sum_{n=0}^{K-k-2}\sum_{m=0}^{k-1}\sum_{i=5}^{6} \frac{\varsigma_i \varepsilon_B \chi_3}{(K-k)\left(\frac{r_F}{r_B}\right)^\alpha + \varepsilon_B}$, $\chi_3 = ((K + \varpi_i)\chi_1 + \chi_2)^{-N}$,

$\varpi = [0, 0, n+2, 1, m+1-k, -k]$, $P_{out,3}^{K-1,\infty} \approx \sum_{n=0}^{K-2} \mu_4 \sum_{j=3}^{4} (-1)^{j+1} \varepsilon_B \left(\frac{1-\chi_4}{\varpi_j r_B^{-\alpha} + r_F^{-\alpha}\varepsilon_B} + \frac{\chi_4}{r_B^{-\alpha} + r_F^{-\alpha}\varepsilon_B}\right)$,

$\mu_4 = \frac{K!(-1)^n \binom{K-2}{n}}{(K-2)!(n+1)}$, and $\chi_4 = (\varpi_j \chi_1 + \chi_2)^{-N}$.

Proof. See Appendix F. □

Remark 13. *For the SGF systems with multiple GF users, when $\rho_B = \rho_F \to \infty$, it must be noted that there is $\Pr\left\{\rho_F |h_k|^2 < \tau\left(|h_B|^2\right)\right\} = \Pr\left\{|h_k|^2 < \frac{|h_B|^2}{\varepsilon_B}\right\}$. The number of the users in*

Groups I and II depends on the relationship between $\frac{|g_k|^2}{r_F^\alpha}$ and $\frac{|h_B|^2}{\varepsilon_B} = \frac{|g_B|^2}{r_B^\alpha\left(2^{R_B}-1\right)}$ irrelated to ρ_B and ρ_F.

Remark 14. *Based on **Corollary 4**, one can observe that when $\rho_B = \rho_F \to \infty$, the SOP of the SGF systems with multiple GF users is a constant, which depends on R_B, R_{th}, r_B, r_F, r_E, and K. Further, $P_{out,3}$ is the main part of the SOP.*

Remark 15. *Based on **Corollaries** 3 and 4, one can find that varying transmit power at U_B and U_F can only improve the secrecy performance of the SGF systems within a certain range. In contrast, improving the system's secrecy performance is more effective by varying the distance. Specifically, reducing the distance between the GF users and the base station as much as possible or making the GF users far from the eavesdroppers. All the parameters must be carefully chosen to maximize the secrecy performance of the considered SGF systems, such as the target rate of U_B, the secrecy threshold rate of U_F, and the distance between the transmitters and receivers.*

V. NUMERICAL RESULTS AND DISCUSSIONS

This section presents Monte-Carlo simulations and numerical results to prove the secrecy performance analysis on the NOMA-aided SGF systems through varying parameters, such as transmit SNR, target data rate, and the number of antennas, etc. The main parameters are set as R_{th} = 0.1, R_B = 0.9, $N = 2$, $\alpha = 2.2$, $r_B = r_F = r_E = 10$ m, unless stated otherwise. In all the figures, "Sim", "Ana", and " Asy" denote the simulation, numerical results, and asymptotic analysis respectively. The results in all the figures demonstrate that the analytical results perfectly match the simulation results, verifying our analysis's accuracy.

A. SOP of the NOMA-aided SGF system with a single-GF-user

Fig. 2 demonstrates the SOP of the single-GF-user NOMA-aided SGF system with varying ρ_B. One can easily observe that the SOP increases initially and subsequently decreases with increasing ρ_B. This is because α_B decreases as ρ_B increases, then the probability that the signals from U_F are decoded first decreases for a given ρ_F. In the lower-ρ_B region, the interference power tolerated for the U_B is limited, so the signals from U_F are always decoded first to ensure the QoS of U_B. The achievable rate for U_F (R_F^{I}) decreases with increasing of ρ_B while the eavesdropping rate is independent of ρ_B; thus, the secrecy performance deteriorates. As the ρ_B increases, τ_B increases, whereas the probability of decoding signals from U_F during the first
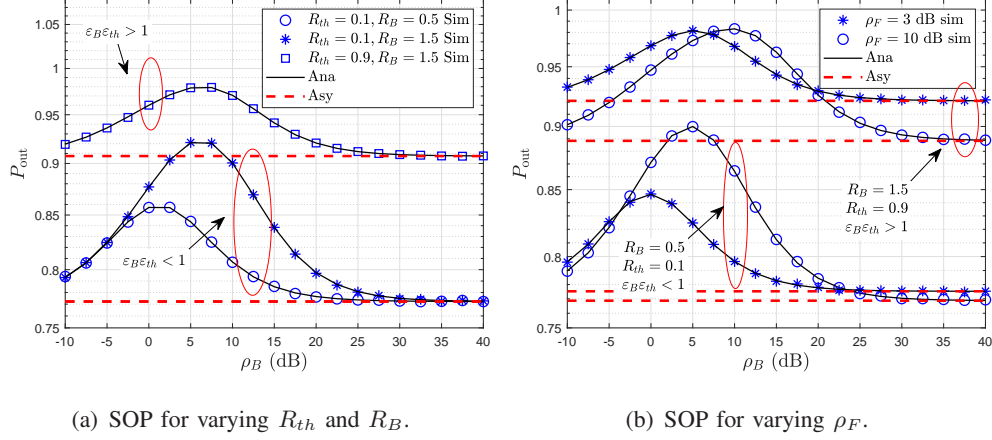
(a) SOP for varying R_{th} and R_B.

(b) SOP for varying ρ_F.

Fig. 2: SOP of the single-GF-user NOMA-aided SGF system with respect to $\epsilon_B \epsilon_{th}$ under varying ρ_B.

(a) SOP for varying R_{th} and R_B.
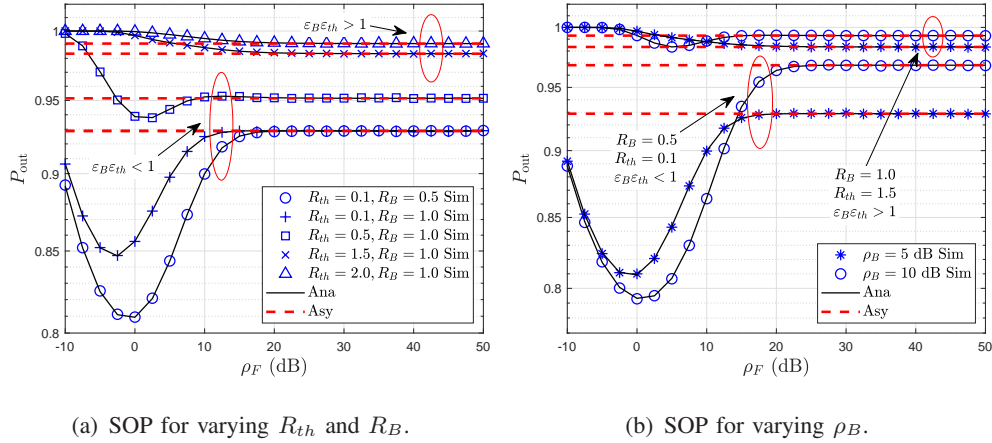
(b) SOP for varying ρ_B.

Fig. 3: SOP of the single-GF-user NOMA-aided SGF system with respect to $\epsilon_B \epsilon_{th}$ under varying ρ_F .

stage of SIC decreases. In the larger-ρ_B region, SOP tends to be a constant, independent of ρ_B but depends on ρ_F and R_{th}. Moreover, the effect from R_{th} is relatively larger than that from R_B since R_B only affects τ_B, i.e., the probability of decoding x_F first, while R_{th} not only affects the probability of decoding x_F first but also affects the achievable rate for U_F (R_F^{I}).

Figs. 3 describes SOP of U_F with varying ρ_F. One can observe that SOP in the larger-ρ_F region tends to be a constant. This is because the probability of decoding signals from U_F during the first stage of SIC increases with increasing ρ_F, i.e. $\Pr\left\{\rho_F|h_F|^2 > \tau\left(|h_B|^2\right)\right\} \rightarrow 1$. Thus, we have $P_{out}^{\mathrm{II}} \rightarrow 0$ and $P_{out} = P_{out}^{\mathrm{I}} = \Pr\left\{R_s^{\mathrm{I}} < R_{th}\right\}$, which depends on R_{th} and ρ_B.
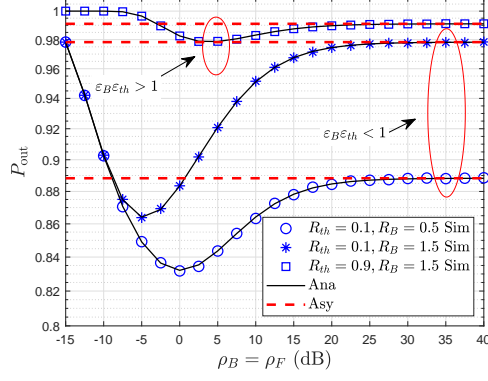
Fig. 4: SOP of the single-GF-user NOMA-aided SGF system with respect to $\epsilon_B\epsilon_{th}$ under increasing $\rho_B = \rho_F$.

Further, the SOP trends in the lower-ρ_F region vary with different $\varepsilon_B\varepsilon_{th}$. Specifically, when $\varepsilon_B\varepsilon_{th} > 1$, SOP decreases with increasing ρ_F. For the case with $\varepsilon_B\varepsilon_{th} < 1$ in lower-ρ_F region, SOP firstly decreases, then increases to a constant. An important factor is the probability of decoding during the first or second stage, which depends on ρ_F, ρ_B, and α_B. As ρ_F increases or/and α_B increases, the probability of first decoding increases, and SOP increases. As ρ_B and τ_B increase, the probability of first decoding decreases, then SOP decreases, as shown in Fig. 3.

Fig. 4 demonstrates SOP versus varying $\rho_B = \rho_F$ simultaneously. One can observe that SOP of U_F is enhanced and then becomes worse until it tends to a constant depending on R_B and R_{th} with increasing $\rho_B = \rho_F$. This is because ρ_F affects both the signal-to-interference-noise ratio (SINR) at U_B and SNR at E while ρ_B only influences the SINR at U_B. Thus, ρ_F has a stronger effect on SOP relative to ρ_B when $\rho_B = \rho_F$ vary simultaneously. Furthermore, when $\rho_B = \rho_F$ vary in a smaller range simultaneously, SOP depends mainly on R_{th}. There is an optimal transmit SNR depending on R_B and R_{th} to obtain the minimum SOP in these scenarios.

B. SOP of the NOMA-aided SGF system with multiple GF users

Figs. 5 and 6 demonstrate the impact of various K, R_B, and R_{th} on SOP of U_F. As can be observed from the figure, with the increase of ρ_B, SOP first increases and then decreases to a constant depending on K and R_{th}. Moreover, with an increase in K, the SOP improves since the better GF user is selected to access the channel, enhancing the secrecy performance. Based on Figs. 5 and 6, one can observe that the effect of the transmit SNR, ρ_B, and ρ_F, on the SOP with multiple GF users is similar to that in Figs. 2 - 3 with a single GF user.
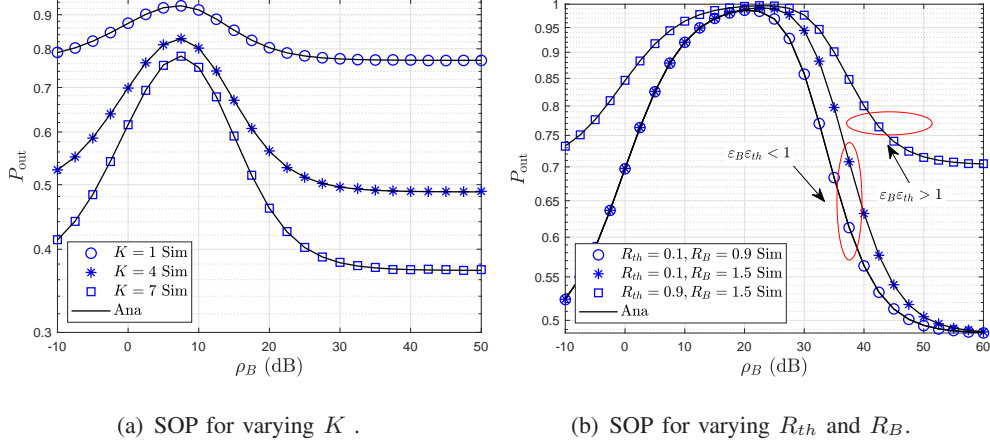
(a) SOP for varying K .

(b) SOP for varying R_{th} and R_B.

Fig. 5: SOP of the multiple-GF-user NOMA-aided SGF system experiencing $\rho_F = 10$ dB .

(a) SOP for varying K.
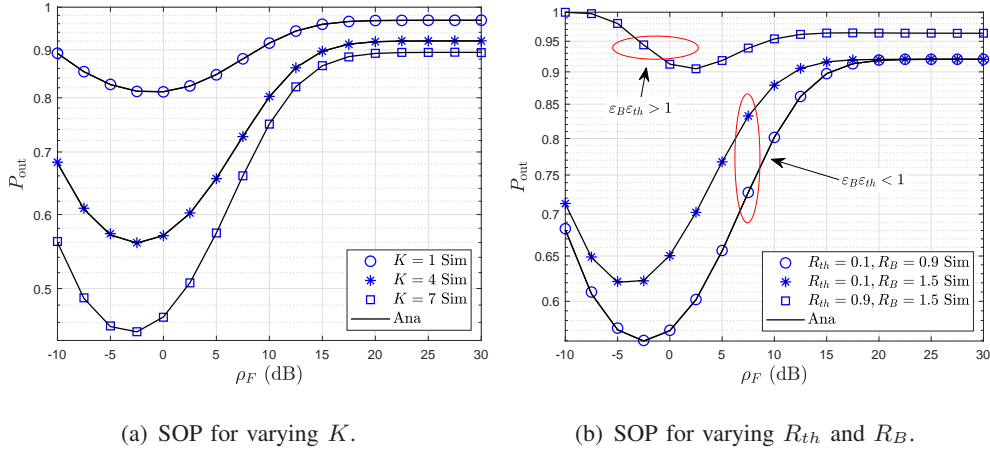
(b) SOP for varying R_{th} and R_B.

Fig. 6: SOP of the multiple-GF-user NOMA-aided SGF system experiencing $\rho_B = 10$ dB.

Fig. 7 plots the effects of varying K, R_B, R_{th}, and N on SOP versus varying $\rho_B = \rho_F$ One can observe that the curves of SOP in these scenarios are similar to those demonstrated in Fig. 4. Moreover, from Fig. 7(c), one can observe that SOP of U_F becomes worse until it tends to be a constant depending on N. This can be explained by the fact that weakening diversity at E implies a better security performance of the considered SGF system.

Comparing Figs. (2) and (5), (3) and (6), one interesting conclusion can be drawn that the transmit power of the GF and GB users has an opposite impact on the GF user' secrecy performance. From the point of view of security of GF users, there exists an optimal P_F and a worst P_B.
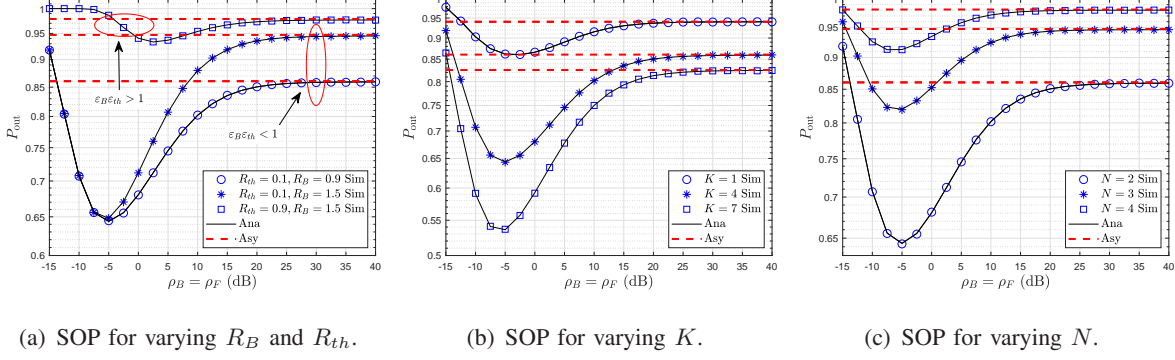
(a) SOP for varying R_B and R_{th}.

(b) SOP for varying K.

(c) SOP for varying N.

Fig. 7: SOP of the multiple-GF-user NOMA-aided SGF system versus varying $\rho_B = \rho_F$.

(a) SOP for varying r_B.

(b) SOP for varying r_F.
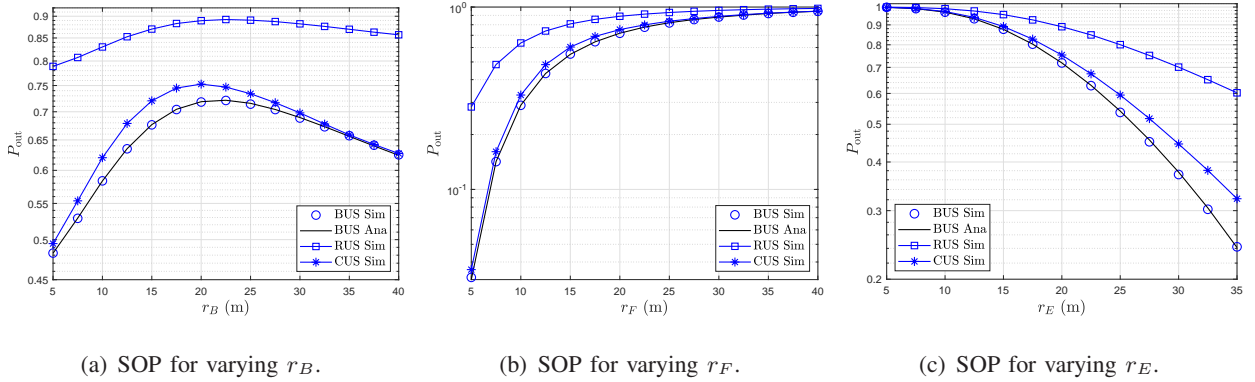
(c) SOP for varying r_E.

Fig. 8: SOP of the multiple-GF-user NOMA-aided SGF system for different user scheduling schemes with $\rho_B = \rho_F = 5$ dB.

Fig. 8 demonstrates the NOMA-aided SGF system for different user scheduling schemes with varying r_B, r_F, and r_E. From Fig. 8(a), one can observe that the SOP increases initially and subsequently decreases with increasing r_B. The achievable rate for U_F decreases with increasing r_B thereby the secrecy performance deteriorates. As the r_B increases, τ_B increases, whereas the probability of decoding signals from U_F during the second stage of SIC increases. Thus, security of U_F with all the schemes is enhanced. Figs. 8(b) and 8(c) demonstrate that r_F and r_E have an opposite impact on the GF user's secrecy performance, which is easy to follow. Furthermore, the BUS scheme obtains the best security while the RUS scheme obtains the worst secrecy performance. This is because the GF user with maximum data rate is scheduled to transmit signals in the BUS scheme while a GF user is selected randomly in the RUS scheme. Moreover, it can be observed that the difference between the secrecy performance with the BUS

and CUS schemes is minor in the lower/larger-r_B region (Fig. 8(a)) and lower/larger-r_F (Fig. 8(b)). The reason is as follows. The CUS scheme is proposed to solve the fairness between GF users due to the difference in path loss in each group. In the scenarios with lower/larger-r_B region (Fig. 8(a)) or lower/larger-r_F (Fig. 8(b)), the GF users belong to the same group with high probability. Assuming the same distance between the GF user and the base station, the user with the maximum power gain leads to the maximum rate. Thus, the secrecy performance with BUS and CUS schemes is equal.

VI. CONCLUSION

In this paper, we investigated the secrecy outage performance of the NOMA-aided SGF systems. With the premise that GF users are entirely transparent for GB users, we first analyzed the NOMA-aided SGF system with a single GF user. Subsequently, the secrecy performance of NOMA-aided SGF systems with multiple GF users was investigated. The effects of all the parameters, such as the target data rate of GB users, the secrecy threshold rate of GF users, and transmit powers on GB and GF users, were discussed. Monte-Carlo simulation results were presented to validate the correctness of the derived analytical expressions.

SIC and CSI are assumed to be perfect in this work, which is a typical assumption in many works, like [9]-[13]. The performance results assuming perfect SIC can be seen as an upper bound of the case with imperfect SIC and worst-case SIC, respectively. An exciting direction for future research is investigating the performance of NOMA-aided SGF systems with imperfect SIC and CSI. In this work, it assumed that all users transmit at fixed power. However, the results in [17] and [18] showed that the system performance could be enhanced by carefully adjusting the transmit power of the GF and GB users. As we analyzed previously, there exists an optimal P_F and a worst P_B for the security of GF users. Thus, analyzing the secrecy performance of the NOMA-based SGF systems wherein both the transmit powers of the GB and GF users are dynamically adjusted in a coordinated manner will be exciting subsequent work. To facilitate performance analysis, it is assumed that all the GF users are located in a small cluster, such that the distances between GF users and the base station are the same. Another interesting problem is analyzing the performance of NOMA-aided SGF systems with multiple randomly distributed GB users, GF users, and eavesdroppers via stochastic geometry. Furthermore, machine-type GF users in mMTC applications often have small data packets. Fairness is another issue that is

as important as security. Analyzing the secrecy performance of NOMA-based SGF systems for short-packet transmission with the different user scheduling schemes also is an exciting problem.

APPENDIX A
PROOF OF THEOREM 1

A. Derivation of P_{out}^{I}

Based on the definition of $\tau\left(|h_B|^2\right)$, P_{out}^{I} is expressed as

$$
\begin{aligned}
P_{out}^{\mathrm{I}} &= \Pr\left\{R_s^{\mathrm{I}} < R_{th}, \rho_F|h_F|^2 > \tau\left(|h_B|^2\right), \tau\left(|h_B|^2\right) < 0\right\} \\
&\quad + \Pr\left\{R_s^{\mathrm{I}} < R_{th}, \rho_F|h_F|^2 > \tau\left(|h_B|^2\right), \tau\left(|h_B|^2\right) > 0\right\} \\
&= \Pr\left\{R_s^{\mathrm{I}} < R_{th}, \rho_F|h_F|^2 > 0, |h_B|^2 < \alpha_B\right\} \\
&\quad + \Pr\left\{R_s^{\mathrm{I}} < R_{th}, \rho_F|h_F|^2 > \tau_B, |h_B|^2 > \alpha_B\right\} \\
&= \underbrace{\Pr\left\{R_s^{\mathrm{I}} < R_{th}, |h_B|^2 < \alpha_B\right\}}_{P_{out}^{\mathrm{I},1}} + \underbrace{\Pr\left\{R_s^{\mathrm{I}} < R_{th}, |h_F|^2 > \frac{\tau_B}{\rho_F}, |h_B|^2 > \alpha_B\right\}}_{P_{out}^{\mathrm{I},2}}.
\end{aligned} \tag{A.1}
$$

In (A.1), $P_{out}^{\mathrm{I},1}$ denotes the SOP of U_F when U_B is in outage while accessing the channel alone. In these scenarios, S can not successfully decode the signals from U_B while decoding signals from U_F is a unique choice. $P_{out}^{\mathrm{I},2}$ signifies SOP of U_F when U_B is not in outage while accessing the channel alone. In this scenario, although S can successfully decode the signals from U_B, the QoS of U_B cannot be guaranteed because of the interference caused by U_F. Therefore, the signals from U_F must be decoded at the first stage of SIC.

Substituting (10) into (A.1) and after some algebraic manipulations, we obtain

$$P_{out}^{I,1} = \Pr\left\{\log_2\left(1 + \frac{\rho_F|h_F|^2}{1 + \rho_B|h_B|^2}\right) - \log_2\left(1 + \rho_F|H_E|^2\right) < R_{th}, |h_B|^2 < \alpha_B\right\}$$

$$= \Pr\left\{|h_F|^2 < \underbrace{\rho_B\theta_{th}|h_B|^2|H_E|^2 + \theta_{th}|H_E|^2 + \rho_B\alpha_{th}|h_B|^2 + \alpha_{th}}_{\triangleq \omega_0\left(|h_B|^2, |H_E|^2\right)}, |h_B|^2 < \alpha_B\right\}$$

$$= \int_0^\infty \int_0^{\alpha_B} F_{|h_F|^2}\left(\omega_0\left(x,y\right)\right) f_{|h_B|^2}\left(x\right) dx f_{|H_E|^2}\left(y\right) dy \tag{A.2}$$

$$= \frac{r_B^\alpha r_E^{N\alpha}}{\Gamma\left(N\right)} \int_0^\infty y^{N-1} e^{-r_E^\alpha y} \int_0^{\alpha_B} e^{-r_B^\alpha x} dx dy$$

$$- \frac{r_B^\alpha r_E^{N\alpha} e^{-r_F^\alpha \alpha_{th}}}{\Gamma\left(N\right)} \int_0^\infty \int_0^{\alpha_B} y^{N-1} e^{-\lambda_1 xy - \lambda_2 x - \lambda_3 y} dx dy$$

$$= 1 - e^{-r_B^\alpha \alpha_B} - \frac{r_B^\alpha r_E^{N\alpha} e^{-r_F^\alpha \alpha_{th}} \omega_1\left(\lambda_1, \lambda_2, \lambda_3\right)}{\Gamma\left(N\right)},$$

where $\omega_1\left(a, b, c\right) \overset{(a)}{=} \frac{b^{N-1}\Gamma(N)}{a^N} e^{\frac{bc}{a}} \left(\Gamma\left(1 - N, \frac{bc}{a}\right) - \Gamma\left(1 - N, b\alpha_B + \frac{bc}{a}\right)\right)$, $\alpha_{th} = \frac{\varepsilon_{th}}{\rho_F}$, $\varepsilon_{th} = \theta_{th} - 1$, $\theta_{th} = 2^{R_{th}}$, $\lambda_1 = r_F^\alpha \rho_B \theta_{th}$, $\lambda_2 = r_F^\alpha \rho_B \alpha_{th} + r_B^\alpha$, $\lambda_3 = r_F^\alpha \theta_{th} + r_E^\alpha$, and (a) is obtained via utilizing [30, (3.383.10)].

Similarly, we obtain

$$P_{out}^{I,2} = \Pr\left\{|h_F|^2 < \omega_0\left(|h_B|^2, |H_E|^2\right), |h_F|^2 > \frac{\tau_B}{\rho_F}, |h_B|^2 > \alpha_B\right\}. \tag{A.3}$$

The relationship between $\omega_0\left(|h_B|^2, |H_E|^2\right)$ and $\frac{\tau_B}{\rho_F}$ is expressed as

$$\Pr\left\{\frac{\tau_B}{\rho_F} < \omega_0\left(|h_B|^2, |H_E|^2\right)\right\} = \Pr\left\{1 - \varepsilon_B\varepsilon_{th} - \varepsilon_B\rho_F\theta_{th}|H_E|^2 < 0\right\}$$

$$+ \Pr\left\{1 - \varepsilon_B\varepsilon_{th} - \varepsilon_B\rho_F\theta_{th}|H_E|^2 > 0, |h_B|^2 < \alpha_2\right\} \tag{A.4}$$

$$= \Pr\left\{|H_E|^2 > \alpha_1\right\} + \Pr\left\{|H_E|^2 < \alpha_1, |h_B|^2 < \alpha_2\right\},$$

where $\theta_B = 2^{R_B}$, $\alpha_1 = \frac{1 - \varepsilon_B\varepsilon_{th}}{\rho_F\theta_{th}\varepsilon_B}$, $\alpha_2 = \frac{\rho_F\varepsilon_1|H_E|^2 + \varepsilon_1}{-\rho_F\theta_{th}\varepsilon_B|H_E|^2 + 1 - \varepsilon_B\varepsilon_{th}} = \frac{\alpha_3}{\alpha_1 - |H_E|^2} - \frac{1}{\rho_B}$, $\varepsilon_1 = \alpha_B\theta_{th}$, and $\alpha_3 = \frac{\theta_B}{\rho_F\theta_{th}\rho_B\varepsilon_B}$. Eq. (A.4) is easy to follow, while the first item denotes the scenario that the eavesdropper link is too strong and the second term denotes that the eavesdropper link is relatively weak and there is a constraint on the GB link from the eavesdropper link. Moreover, the relationship α_1 and 0 has important effect on the relationship between $\omega_0\left(|h_B|^2, |H_E|^2\right)$ and $\frac{\tau_B}{\rho_F}$.

(i) When $\varepsilon_B \varepsilon_{th} < 1$, we have $\alpha_1 > 0$. Then, based on (A.3), $P_{out}^{\mathrm{I},2}$ is obtained as

$$
\begin{aligned}
P_{out}^{\mathrm{I},21} &= \Pr\left\{ |h_F|^2 < \omega_0\left(|h_B|^2, |H_E|^2\right), |h_F|^2 > \frac{\tau_B}{\rho_F}, |h_B|^2 > \alpha_B \right\} \\
&= \Pr\left\{ \frac{\tau_B}{\rho_F} < |h_F|^2 < \omega_0\left(|h_B|^2, |H_E|^2\right), |h_B|^2 > \alpha_B, |H_E|^2 > \alpha_1 \right\} \\
&+ \Pr\left\{ \frac{\tau_B}{\rho_F} < |h_F|^2 < \omega_0\left(|h_B|^2, |H_E|^2\right), \alpha_B < |h_B|^2 < \alpha_2, |H_E|^2 < \alpha_1 \right\} \\
&= \frac{e^{-r_B^\alpha \alpha_B} r_B^\alpha \Gamma\left(N, r_E^\alpha \alpha_1\right)}{\varepsilon_2 \Gamma(N)} + e^{\frac{r_F^\alpha}{\rho_F}} r_B^\alpha r_E^{N\alpha} \frac{\omega_3\left(0, \varepsilon_2, r_E^\alpha\right)}{\Gamma(N)} \\
&- e^{-r_F^\alpha \alpha_{th}} r_B^\alpha r_E^{N\alpha} \frac{\omega_2\left(\lambda_1, \lambda_2, \lambda_3\right) + \omega_3\left(\lambda_1, \lambda_2, \lambda_3\right)}{\Gamma(N)},
\end{aligned}
\tag{A.5}
$$

where

$$
\begin{aligned}
\omega_2\left(a, b, c\right) &= \int_{\alpha_1}^{\infty} \int_{\alpha_B}^{\infty} y^{N-1} e^{-axy - bx - cy} dx\, dy \\
&\overset{(b)}{=} \frac{b^{N-1}\Gamma(N)}{a^N} e^{\frac{bc}{a}} \Gamma\left(1 - N, b\alpha_B + \frac{bc}{a}\right) - e^{-b\alpha_B}\Delta,
\end{aligned}
\tag{A.6}
$$

$$
\Delta = \int_0^{\alpha_1} \frac{y^{N-1} e^{-(a\alpha_B + c)y}}{ay + b} dy \overset{(c)}{=} \frac{\pi \alpha_1}{2R} \sum_{r=1}^{R} \frac{\sqrt{1 - \ell_r^2}}{a\hbar_r + b} \hbar_r^{N-1} e^{-(a\alpha_B + c)\hbar_r},
\tag{A.7}
$$

and

$$
\begin{aligned}
\omega_3\left(a, b, c\right) &= \int_0^{\alpha_1} \frac{y^{N-1} e^{-(a\alpha_B + c)y}}{ay + b} dy - e^{\frac{b}{P_B} - a\alpha_3} \int_0^{\alpha_1} \frac{y^{N-1} e^{\left(\frac{a}{P_B} - c\right)y - \frac{\alpha_3(a\alpha_1 + b)}{y - \alpha_1}}}{ay + b} dy \\
&\overset{(d)}{=} \frac{b^{N-1}\Gamma(N)}{a^N} e^{\frac{bc}{a}} \Gamma\left(1 - N, b\alpha_B + \frac{bc}{a}\right) - \omega_2\left(a, b, c\right) \\
&- e^{\frac{b}{P_B} - a\alpha_3} \frac{\pi \alpha_1}{2L} \sum_{l=1}^{L} \frac{\sqrt{1 - \vartheta_l^2}}{av_l + b} v_l^{N-1} e^{\left(\frac{a}{P_B} - c\right)v_l - \frac{\alpha_3(a\alpha_1 + b)}{\alpha_1 - v_l}},
\end{aligned}
\tag{A.8}
$$

$\varepsilon_2 = \frac{r_F^\alpha}{P_F \alpha_B} + r_B^\alpha$, (b) holds by applying [30, (3.383.10)], and (c) and (d) holds by [30, (3.383.10)] and applying Gaussian-Chebyshev quadrature [31, (25.4.30)], R and L is the summation item, which reflects accuracy vs. complexity, $\ell_r = \cos\left(\frac{2r-1}{2R}\pi\right)$, $\hbar_r = \frac{\alpha_1}{2}\left(\ell_r + 1\right)$, $\vartheta_l = \cos\left(\frac{2l-1}{2L}\pi\right)$, and $v_l = \frac{\alpha_1}{2}\left(\vartheta_l + 1\right)$.

(ii) When $\varepsilon_B \varepsilon_{th} > 1$, it has $\alpha_1 < 0$, then, $\Pr\left\{\frac{\tau_B}{\rho_F} < \omega_0\left(|h_B|^2, |H_E|^2\right)\right\} = \Pr\left\{|H_E|^2 > \alpha_1\right\} = 1$. Thus, $P_{out}^{I,2}$ is expressed as

$$
\begin{aligned}
P_{out}^{I,22} &= \Pr\left\{\frac{\tau_B}{\rho_F} < |h_F|^2 < \omega_0\left(|h_B|^2, |H_E|^2\right), |h_B|^2 > \alpha_B\right\} \\
&= \int_0^\infty \int_{\alpha_B}^\infty \left(F_{|h_F|^2}\left(\omega_0\left(x,y\right)\right) - F_{|h_F|^2}\left(\frac{\tau_B}{\rho_F}\right)\right) f_{|h_B|^2}(x)\, dx f_{|H_E|^2}(y)\, dy \\
&= \frac{r_B^\alpha r_E^{N\alpha} e^{\frac{r_F^\alpha}{\rho_F}}}{\Gamma(N)} \int_0^\infty \int_{\alpha_B}^\infty y^{N-1} e^{-\varepsilon_2 x - r_E^\alpha y}\, dx\, dy \\
&\quad - \frac{r_B^\alpha r_E^{N\alpha} e^{-r_F^\alpha \alpha_{th}}}{\Gamma(N)} \int_0^\infty \int_{\alpha_B}^\infty y^{N-1} e^{-\lambda_1 xy - \lambda_2 x - \lambda_3 y}\, dx\, dy \\
&= \frac{r_B^\alpha e^{-r_B^\alpha \alpha_B}}{\varepsilon_2} - \frac{r_B^\alpha r_E^{N\alpha} e^{-r_F^\alpha \alpha_{th}} \omega_4\left(\lambda_1, \lambda_2, \lambda_3\right)}{\Gamma(N)},
\end{aligned}
$$
(A.9)

where

$$
\begin{aligned}
\omega_4(a,b,c) &= \int_0^\infty \int_{\alpha_B}^\infty y^{N-1} e^{-axy - bx - cy}\, dx\, dy \\
&\overset{(e)}{=} \frac{b^{N-1}\Gamma(N)}{a^N} e^{\frac{bc}{a}} \Gamma\left(1 - N, b\alpha_B + \frac{bc}{a}\right),
\end{aligned}
$$
(A.10)

step (e) is obtained by applying [30, (3.383.10)].

B. Derivation of P_{out}^{II}

Similar to (A.1), P_{out}^{II} is expressed as

$$
\begin{aligned}
P_{out}^{II} &= \Pr\left\{R_s^{II} < R_{th}, \rho_F|h_F|^2 < 0, |h_B|^2 < \alpha_B\right\} + \Pr\left\{R_s^{II} < R_{th}, \rho_F|h_F|^2 < \tau_B, |h_B|^2 > \alpha_B\right\} \\
&= \Pr\left\{R_s^{II} < R_{th}, |h_F|^2 < \frac{\tau_B}{\rho_F}, |h_B|^2 > \alpha_B\right\} \\
&= \Pr\left\{|h_F|^2 < \theta_{th}|H_E|^2 + \alpha_{th}, |h_F|^2 < \frac{\tau_B}{\rho_F}, |h_B|^2 > \alpha_B\right\}.
\end{aligned}
$$
(A.11)

In this case, the relationship between constraint on security $(\theta_{th}|H_E|^2 + \alpha_{th})$ and constraint on decoding order is considered as follow.

$$
\Pr\left\{\frac{\tau_B}{\rho_F} < \theta_{th}|H_E|^2 + \alpha_{th}\right\} = \Pr\left\{|h_B|^2 < \left(\rho_F|H_E|^2 + 1\right)\varepsilon_1\right\}.
$$
(A.12)

Due to $\theta_{th} = 2^{R_{th}} \geqslant 1$, then $\Pr\left\{\left(\rho_F|H_E|^2 + 1\right)\varepsilon_1 > \alpha_B\right\} = 1$. Thus, P_{out}^{II} is obtained as

$$
\begin{aligned}
P_{out}^{\text{II}} &= \Pr\left\{|h_F|^2 < \theta_{th}|H_E|^2 + \alpha_{th}, |h_B|^2 > \left(\rho_F|H_E|^2 + 1\right)\varepsilon_1\right\} \\
&\quad + \Pr\left\{|h_F|^2 < \frac{\tau_B}{\rho_F}, \alpha_B < |h_B|^2 < \left(\rho_F|H_E|^2 + 1\right)\varepsilon_1\right\} \\
&= \int_0^\infty \int_{(\rho_F y + 1)\varepsilon_1}^\infty F_{|h_F|^2}\left(\theta_{th}y + \alpha_{th}\right) f_{|h_B|^2}(x)\, dx\, f_{|H_E|^2}(y)\, dy \\
&\quad + \int_0^\infty \int_{\alpha_B}^{(\rho_F y + 1)\varepsilon_1} F_{|h_F|^2}\left(\frac{\tau_B}{\rho_F}\right) f_{|h_B|^2}(x)\, dx\, f_{|H_E|^2}(y)\, dy \\
&= \frac{r_E^{N\alpha} r_B^\alpha}{\Gamma(N)} \int_0^\infty \int_{(\rho_F y + 1)\varepsilon_1}^\infty \left(1 - e^{-r_F^\alpha(\theta_{th}y + \alpha_{th})}\right) e^{-r_B^\alpha x} y^{N-1} e^{-r_E^\alpha y} dx\, dy \\
&\quad + \frac{r_E^{N\alpha} r_B^\alpha}{\Gamma(N)} \int_0^\infty \int_{\alpha_B}^{(\rho_F y + 1)\varepsilon_1} \left(1 - e^{-r_F^\alpha\left(\frac{x}{P_F \alpha_B} - \frac{1}{P_F}\right)}\right) e^{-r_B^\alpha x} y^{N-1} e^{-r_E^\alpha y} dx\, dy \\
&= \frac{r_F^\alpha e^{-r_B^\alpha \alpha_B}}{r_B^\alpha P_F \alpha_B + r_F^\alpha} - \frac{r_E^{N\alpha} r_F^\alpha e^{-\left(r_F^\alpha \alpha_{th} + r_B^\alpha \varepsilon_1\right)}}{\left(r_F^\alpha \rho_F \alpha_B + r_B^\alpha\right)\left(r_B^\alpha \rho_F \varepsilon_1 + \lambda_3\right)^N}.
\end{aligned}
\tag{A.13}
$$

Substituting (A.2), (A.5), (A.9), (A.13) into (11), we have (13).

APPENDIX B

PROOF OF COROLLARY 1

When $\rho_B \to \infty$, we have $\alpha_B = \frac{\varepsilon_B}{\rho_B} \to 0$. Based on (11), we obtain $\tau_B \to \infty$, then $P_{out}^{\text{I}} \approx 0$ and P_{out}^{II} is approximated as

$$
\begin{aligned}
P_{out}^{\text{II},\rho_B \to \infty} &\approx \Pr\left\{R_s^{\text{II}} < R_{th}\right\} \\
&= \Pr\left\{|h_F|^2 < \theta_{th}|H_E|^2 + \alpha_{th}\right\} \\
&= \int_0^\infty F_{|h_F|^2}\left(\theta_{th}x + \alpha_{th}\right) f_{|H_E|^2}(x)\, dx \\
&= 1 - e^{-r_F^\alpha \alpha_{th}}\left(1 + \theta_{th}\left(\frac{r_F}{r_E}\right)^\alpha\right)^{-N}.
\end{aligned}
\tag{B.1}
$$

APPENDIX C

PROOF OF COROLLARY 2

When $\rho_F \to \infty$, based on (11), we can easily observe $P_{out}^{\mathrm{II}} \approx 0$ and P_{out}^{I} is expressed as

$$
\begin{aligned}
P_{out}^{\mathrm{I},\rho_F\to\infty} &= \Pr\left\{R_s^{\mathrm{I}} < R_{th}\right\} \\
&\approx \Pr\left\{|h_F|^2 < \left(\rho_B\theta_{th}|h_B|^2 + \theta_{th}\right)|H_E|^2\right\} \\
&= \int_0^\infty \int_0^\infty F_{|h_F|^2}\left(\left(\rho_B\theta_{th}x + \theta_{th}\right)y\right)f_{|h_B|^2}(x)\,f_{|H_E|^2}(y)\,dxdy \\
&= 1 - \left(\frac{r_B}{r_F}\right)^{N\alpha}\left(\frac{r_E^\alpha}{\rho_B\theta_{th}}\right)^N \Gamma\left(1 - N, \frac{r_B^\alpha}{\rho_B\theta_{th}}\left(\theta_{th} + \left(\frac{r_E}{r_F}\right)^\alpha\right)\right).
\end{aligned}
\tag{C.1}
$$

APPENDIX D

PROOF OF COROLLARY 3

When $\rho_B = \rho_F \to \infty$, we have $\frac{r_B}{\rho_F} \to \frac{|h_B|^2}{\varepsilon_B}$. Based on (11), P_{out}^{I} is approximated as

$$
\begin{aligned}
P_{out}^{\mathrm{I},\infty} &\approx \Pr\left\{\frac{|h_B|^2}{\varepsilon_B} < |h_F|^2 < \omega_0\left(|h_B|^2, |H_E|^2\right)\right\} \\
&= \int_0^\infty \int_0^\infty \left(F_{|h_F|^2}\left(\omega_0(x,y)\right) - F_{|h_F|^2}\left(\frac{x}{\varepsilon_B}\right)\right)f_{|h_B|^2}(x)\,dx f_{|H_E|^2}(y)\,dy \\
&\overset{(f)}{\approx} 1 - \frac{1}{1 + \varepsilon_B\left(\frac{r_B}{r_F}\right)^\alpha}.
\end{aligned}
\tag{D.1}
$$

where (f) holds by applying [30, (3.383.10)] and $\Gamma(a,x) \overset{x\to\infty}{\to} 0$. Based on (A.13), P_{out}^{II} is approximated as

$$
\begin{aligned}
P_{out}^{\mathrm{II},\infty} &\approx \Pr\left\{R_s^{\mathrm{II}} < R_{th}, |h_F|^2 < \frac{|h_B|^2}{\varepsilon_B}\right\} \\
&= \Pr\left\{|h_F|^2 < \theta_{th}|H_E|^2, |h_B|^2 > \varepsilon_B\theta_{th}|H_E|^2\right\} \\
&\quad + \Pr\left\{|h_F|^2 < \frac{|h_B|^2}{\varepsilon_B}, |h_B|^2 < \varepsilon_B\theta_{th}|H_E|^2\right\} \\
&= \left(1 + \left(\frac{r_B}{r_F}\right)^\alpha \varepsilon_B\right)^{-1}\left(1 - \left(\left(\frac{r_F}{r_E}\right)^\alpha \theta_{th} + \left(\frac{r_B}{r_E}\right)^\alpha \varepsilon_B\theta_{th} + 1\right)^{-N}\right).
\end{aligned}
\tag{D.2}
$$

APPENDIX E

PROOF OF THEOREM 2

1) *Derivation of $P_{out,1}$*

Based on (17) and $\Pr\left\{\tau\left(|h_B|^2\right) < 0\right\} = \Pr\left\{|h_B|^2 < \alpha_B\right\}$, $P_{out,1}$ is rewritten as

$$P_{out,1} = \underbrace{\Pr\left\{R_K^{\mathrm{I}} - R_E < R_{th}, |S_{\mathrm{II}}| = 0, |h_B|^2 < \alpha_B\right\}}_{\triangleq P_{out,1}^1}$$

$$+ \underbrace{\Pr\left\{R_K^{\mathrm{I}} - R_E < R_{th}, |S_{\mathrm{II}}| = 0, |h_B|^2 > \alpha_B\right\}}_{\triangleq P_{out,1}^2}, \tag{E.1}$$

where $|h_B|^2 < \alpha_B$ denotes U_B is reliability outage. Utilizing [30, (3.383.10)], we obtain

$$
\begin{aligned}
P_{out,1}^1 &= \Pr\left\{R_K^{\mathrm{I}} - R_E < R_{th}, |h_B|^2 < \alpha_B\right\}\\
&= \Pr\left\{\log_2\left(1 + \frac{\rho_F|h_K|^2}{1 + \rho_B|h_B|^2}\right) - \log_2\left(1 + \rho_F|H_E|^2\right) < R_{th}, |h_B|^2 < \alpha_B\right\}\\
&= \Pr\left\{|h_K|^2 < \omega_0\left(|h_B|^2, |H_E|^2\right), |h_B|^2 < \alpha_B\right\}\\
&= \int_0^\infty \int_0^{\alpha_B} F_{|h_K|^2}\left(\omega_0\left(x, y\right)\right) f_{|h_B|^2}\left(x\right) dx f_{|H_E|^2}\left(y\right) dy\\
&= 1 - e^{-r_B^\alpha \alpha_B} + \sum_{i=0}^K \frac{\varphi_i r_B^\alpha r_E^{N\alpha}}{\Gamma\left(N\right)} e^{-ir_F^\alpha \alpha_{th}} \omega_1\left(i\lambda_1, \varepsilon_3, \varepsilon_4\right),
\end{aligned}
\tag{E.2}
$$

where $\varepsilon_3 = ir_F^\alpha \alpha_{th}\rho_B + r_B^\alpha$ and $\varepsilon_4 = ir_F^\alpha \theta_{th} + r_E^\alpha$. Similarly, $P_{out,1}^2$ is expressed as

$$
\begin{aligned}
P_{out,1}^2 &= \Pr\left\{\log_2\left(1 + \frac{\rho_F|h_K|^2}{1 + \rho_B|h_B|^2}\right) - \log_2\left(1 + \rho_F|H_E|^2\right) < R_{th}, |h_1|^2 > \frac{\tau_B}{\rho_F}, |h_B|^2 > \alpha_B\right\}\\
&= \Pr\left\{|h_K|^2 < \omega_0\left(|h_B|^2, |H_E|^2\right), |h_1|^2 > \frac{\tau_B}{\rho_F}, |h_B|^2 > \alpha_B\right\}.
\end{aligned}
\tag{E.3}
$$

Considering $|h_1|^2 \le \cdots \le |h_K|^2$ and the relationship between $\omega_0\left(|h_B|^2, |H_E|^2\right)$ and $\frac{\tau_B}{\rho_F}$, given in (A.4), two scenarios ($\varepsilon_B\varepsilon_{th} < 1$ and $\varepsilon_B\varepsilon_{th} > 1$) are considered as follows.

(i) When $\varepsilon_B\varepsilon_{th} < 1$, we have $\alpha_1 > 0$. Due to $\alpha_B < \alpha_2$, based on (A.4), we obtain

$$
\begin{aligned}
P_{out,1}^{21} &= \Pr\left\{|h_K|^2 < \omega_0\left(|h_B|^2, |H_E|^2\right), |h_1|^2 > \frac{\tau_B}{\rho_F}, |h_B|^2 > \alpha_B\right\}\\
&= \underbrace{\Pr\left\{\frac{\tau_B}{\rho_F} < |h_1|^2 < |h_K|^2 < \omega_0\left(|h_B|^2, |H_E|^2\right), |h_B|^2 > \alpha_B, |H_E|^2 > \alpha_1\right\}}_{I_1}\\
&\quad + \underbrace{\Pr\left\{\frac{\tau_B}{\rho_F} < |h_1|^2 < |h_K|^2 < \omega_0\left(|h_B|^2, |H_E|^2\right), \alpha_B < |h_B|^2 < \alpha_2, |H_E|^2 < \alpha_1\right\}}_{I_2}.
\end{aligned}
\tag{E.4}
$$

Based on (5), we obtain

$$I_1 = \int_{\alpha_1}^{\infty} \int_{\alpha_B}^{\infty} \left(F_{|h_1|^2, |h_K|^2} \left(\frac{\tau_B}{\rho_F}, \omega_0 (x, y) \right) \right) f_{|h_B|^2} (x) \, dx f_{|H_E|^2} (y) \, dy$$

$$= \frac{r_B^{\alpha} r_E^{N\alpha}}{\Gamma(N)} \sum_{n=0}^{K-2} \left(\mu_1 e^{\frac{Kr_F^{\alpha}}{\rho_F}} \omega_2 (0, \alpha_4, r_E^{\alpha}) + \mu_2 e^{-Kr_F^{\alpha}\alpha_{th}} \omega_2 (\eta_1, \eta_2, \eta_3) - \mu_3 e^{\frac{Kr_F^{\alpha} - C_0}{\rho_F} - C_0 \alpha_{th}} \omega_2 (\eta_4, \eta_5, \eta_6) \right),$$
(E.5)

where $\alpha_4 = \frac{Kr_F^{\alpha}}{\rho_F \alpha_B} + r_B^{\alpha}$, $\eta_1 = Kr_F^{\alpha} \rho_B \theta_{th}$, $\eta_2 = Kr_F^{\alpha} \rho_B \alpha_{th} + r_B^{\alpha}$, $\eta_3 = Kr_F^{\alpha} \theta_{th} + r_E^{\alpha}$, $\eta_4 = C_0 \rho_B \theta_{th}$, $\eta_5 = C_0 \rho_B \alpha_{th} + \frac{Kr_F^{\alpha} - C_0}{\rho_F \alpha_B} + r_B^{\alpha}$, and $\eta_6 = C_0 \theta_{th} + r_E^{\alpha}$. Similarly, we obtain

$$I_2 = \int_0^{\alpha_1} \int_{\alpha_B}^{\alpha_2} \left(F_{|h_1|^2, |h_K|^2} \left(\frac{\tau_B}{\rho_F}, \omega_0 (x, y) \right) \right) f_{|h_B|^2} (x) \, dx f_{|H_E|^2} (y) \, dy$$

$$= \frac{r_B^{\alpha} r_E^{N\alpha}}{\Gamma(N)} \sum_{n=0}^{K-2} \left(\mu_1 e^{\frac{Kr_F^{\alpha}}{\rho_F}} \omega_3 (0, \alpha_4, r_E^{\alpha}) + \mu_2 e^{-Kr_F^{\alpha}\alpha_{th}} \omega_3 (\eta_1, \eta_2, \eta_3) - \mu_3 e^{\frac{Kr_F^{\alpha} - C_0}{\rho_F} - C_0 \alpha_{th}} \omega_3 (\eta_4, \eta_5, \eta_6) \right).$$
(E.6)

(ii) When $\varepsilon_B \varepsilon_{th} > 1$, we have $\alpha_1 < 0$, then $\Pr \left\{ \frac{\tau_B}{\rho_F} < \omega_0 \left(|h_B|^2, |H_E|^2 \right) \right\} = 1$. Thus, we obtain

$$P_{out,1}^{22} = \Pr \left\{ \frac{\tau_B}{\rho_F} < |h_1|^2 < |h_K|^2 < \omega_0 \left(|h_B|^2, |H_E|^2 \right), |h_B|^2 > \alpha_B \right\}$$

$$= \int_0^{\infty} \int_{\alpha_B}^{\infty} \left(F_{|h_1|^2, |h_K|^2} \left(\frac{\tau_B}{\rho_F}, \omega_0 (x, y) \right) \right) f_{|h_B|^2} (x) \, dx f_{|H_E|^2} (y) \, dy$$

$$= \frac{r_B^{\alpha} r_E^{N\alpha}}{\Gamma(N)} \sum_{n=0}^{K-2} \left(\mu_1 e^{\frac{Kr_F^{\alpha}}{\rho_F}} \omega_4 (0, \alpha_4, r_E^{\alpha}) + \mu_2 e^{-Kr_F^{\alpha}\alpha_{th}} \omega_4 (\eta_1, \eta_2, \eta_3) - \mu_3 e^{\frac{Kr_F^{\alpha} - C_0}{\rho_F} - C_0 \alpha_{th}} \omega_4 (\eta_4, \eta_5, \eta_6) \right).$$
(E.7)

2) *Derivation of $P_{out,2}$*

When $|\mathcal{S}_{\mathrm{II}}| = K$, U_B's signal must be decoded during the first stage of SIC and the signals of all the GF users will be decoded in the second stage of SIC. Utilizing the best-user scheduling scheme, U_K will be selected. Then, SOP in this case is expressed as

$$P_{out,2} = \Pr \left\{ R_K^{\mathrm{II}} - R_E < R_{th}, |\mathcal{S}_{\mathrm{II}}| = K, |h_B|^2 > \alpha_B \right\}$$

$$= \Pr \left\{ \log_2 \left(1 + \rho_F |h_K|^2 \right) - \log_2 \left(1 + \rho_F |H_E|^2 \right) < R_{th}, |h_K|^2 < \frac{\tau_B}{\rho_F}, |h_B|^2 > \alpha_B \right\}$$

$$= \Pr \left\{ |h_K|^2 < \theta_{th} |H_E|^2 + \alpha_{th}, |h_K|^2 < \frac{\tau_B}{\rho_F}, |h_B|^2 > \alpha_B \right\}$$

$$= \Pr \left\{ |h_K|^2 < \min \left(\frac{\tau_B}{\rho_F}, \theta_{th} |H_E|^2 + \alpha_{th} \right), |h_B|^2 > \alpha_B \right\}$$

$$= \Pr \left\{ |h_K|^2 < \theta_{th} |H_E|^2 + \alpha_{th}, |h_B|^2 > \left(\rho_F |H_E|^2 + 1 \right) \varepsilon_1 \right\}$$

$$+ \Pr \left\{ |h_K|^2 < \frac{\tau_B}{\rho_F}, \alpha_B < |h_B|^2 < \left(\rho_F |H_E|^2 + 1 \right) \varepsilon_1 \right\}.$$
(E.8)

With some simple algebraic manipulations, we obtain

$$P_{out,2} = \sum_{i=0}^{K} \varphi_i \int_0^\infty e^{-i(\theta_{th}y+\alpha_{th})} f_{|H_E|^2}(y) \int_{(\rho_F y+1)\varepsilon_1}^\infty f_{|h_B|^2}(x)\, dxdy$$

$$+ \sum_{i=0}^{K} \varphi_i \int_0^\infty f_{|H_E|^2}(y) \int_{\alpha_B}^{(\rho_F y+1)\varepsilon_1} e^{-\frac{i}{\rho_F}\left(\frac{x}{\alpha_B}-1\right)} f_{|h_B|^2}(x)\, dxdy \qquad \text{(E.9)}$$

$$= \sum_{i=0}^{K} \left(\frac{\varphi_i}{ir_F^\alpha + r_B^\alpha \rho_F \alpha_B} \left(\frac{ir_F^\alpha r_E^{N\alpha} e^{-\left(ir_F^\alpha \alpha_{th}+r_B^\alpha \varepsilon_1\right)}}{\left(ir_F^\alpha \theta_{th} + r_B^\alpha \rho_F \varepsilon_1 + r_E^\alpha\right)^N} + \rho_F \alpha_B r_B^\alpha e^{-r_B^\alpha \alpha_B} \right) \right).$$

3) *Derivation of $P_{out,3}$*

When both $\mathcal{S}_\mathrm{I}$ and $\mathcal{S}_\mathrm{II}$ are not empty, SOP is expressed as

$$P_{out,3} = \sum_{k=1}^{K-2} \underbrace{\Pr\left\{\max\left\{R_K^\mathrm{I}, R_k^\mathrm{II}\right\} - R_E < R_{th}, |S_\mathrm{II}| = k\right\}}_{\triangleq P_{out,3}^k}$$

$$+ \underbrace{\Pr\left\{\max\left\{R_K^\mathrm{I}, R_{K-1}^\mathrm{II}\right\} - R_E < R_{th}, |S_\mathrm{II}| = K-1\right\}}_{\triangleq P_{out,3}^{K-1}}. \qquad \text{(E.10)}$$

Based on (1), (E.1), and (E.8), we have

$$\Pr\left\{|\mathcal{S}_\mathrm{II}| = k, |h_B|^2 > \alpha_B\right\} = \Pr\left\{|h_k|^2 < \frac{\tau_B}{\rho_F} < |h_{k+1}|^2, |h_B|^2 > \alpha_B\right\}, \qquad \text{(E.11)}$$

and

$$\Pr\left\{\max\left\{R_K^\mathrm{I}, R_k^\mathrm{II}\right\} - R_E < R_{th}\right\} = \Pr\left\{|h_k|^2 < \theta_{th}|H_E|^2 + \alpha_{th}, |h_K|^2 < \omega_0\left(|h_B|^2, |H_E|^2\right)\right\}, \qquad \text{(E.12)}$$

respectively. Thus, $P_{out,3}^k$ is expressed as

$$P_{out,3}^k = \Pr\left\{|h_k|^2 < \min\left(\frac{\tau_B}{\rho_F}, \theta_{th}|H_E|^2 + \alpha_{th}\right), |h_B|^2 > \alpha_B,\right.$$

$$\left. \frac{\tau_B}{\rho_F} < |h_{k+1}|^2 < |h_K|^2 < \omega_0\left(|h_B|^2, |H_E|^2\right)\right\}$$

$$= \underbrace{\Pr\left\{|h_k|^2 < \frac{\tau_B}{\rho_F} < |h_{k+1}|^2 < |h_K|^2 < \omega_0\left(|h_B|^2, |H_E|^2\right),\right.}_{I_3}$$
$$\underbrace{\left.\alpha_B < |h_B|^2 < \left(\rho_F|H_E|^2 + 1\right)\varepsilon_1\right\}}_{I_3} \qquad \text{(E.13)}$$

$$+ \underbrace{\Pr\left\{|h_k|^2 < \alpha_{th} + \theta_{th}|H_E|^2, |h_B|^2 > \left(\rho_F|H_E|^2 + 1\right)\varepsilon_1,\right.}_{I_4}$$
$$\underbrace{\left.\frac{\tau_B}{\rho_F} < |h_{k+1}|^2 < |h_K|^2 < \omega_0\left(|h_B|^2, |H_E|^2\right)\right\}}_{I_4}.$$

Based on (7) and utilizing [30, 3.352.2], we obtain

$$
\begin{aligned}
I_3 &= \int_0^\infty f_{|H_E|^2}(t)\, dt \int_{\alpha_B}^{(\rho_F t+1)\varepsilon_1} F_{|h_k|^2,|h_{k+1}|^2|h_K|^2}\left(0,\frac{\tau_B}{\rho_F},\frac{\tau_B}{\rho_F},\omega_0(s,t)\right) f_{|h_B|^2}(s)\, ds \\
&= \sum_{n=0}^{K-k-2}\sum_{m=0}^{k-1}\sum_{i=1}^{6}\varsigma_i \int_0^\infty \int_{\alpha_B}^{(\rho_F t+1)\varepsilon_1} e^{-(B_i+C_i)\frac{\tau_B}{\rho_F}-W_i\omega_0(s,t)} f_{|h_B|^2}(s)\, f_{|H_E|^2}(t)\, ds dt \\
&= \frac{r_B^\alpha r_E^{N\alpha}}{\Gamma(N)}\sum_{n=0}^{K-k-2}\sum_{m=0}^{k-1}\sum_{i=1}^{6}\varsigma_i e^{-\xi_1}\int_0^\infty t^{N-1}e^{-\xi_2 t}\int_{\alpha_B}^{(\rho_F t+1)\varepsilon_1} e^{-(u_1 t+\xi_3)s}\, ds dt \\
&= r_B^\alpha r_E^{N\alpha}\sum_{n=0}^{K-k-2}\sum_{m=0}^{k-1}\left(\sum_{i=1}^{4}\frac{\varsigma_i e^{-\xi_1}}{\Gamma(N)}\Delta_1 + \sum_{i=5}^{6}\varsigma_i e^{-\xi_1}\Delta_2\right),
\end{aligned}
$$

(E.14)

where $\Delta_1 = \frac{\xi_3^{N-1}\Gamma\left(1-N,\xi_3\alpha_B+\frac{\xi_2\xi_3}{u_1}\right)}{u_1^N}e^{\frac{\xi_2\xi_3}{u_1}} - \frac{e^{-\xi_3\varepsilon_1}\omega_5(u_1,\xi_3,v_1,l_1)}{\Gamma(N)}$, $\Delta_2 = \frac{e^{-\xi_3\alpha_B}}{\xi_2^N\xi_3} - \frac{e^{-\xi_3\varepsilon_1}}{\xi_3(\rho_F\xi_3\varepsilon_1+\xi_2)^N}$, $\xi_1 = W_i\alpha_{th} - \frac{B_i+C_i}{\rho_F}$, $\xi_2 = W_i\theta_{th}+r_E^\alpha$, $\xi_3 = W_i\rho_B\alpha_{th}+\frac{B_i+C_i}{P_F\alpha_B}+r_B^\alpha$, $u_1 = W_i\rho_F\theta_{th}$, $v_1 = u_1\rho_F\varepsilon_1$, $l_1 = u_1\varepsilon_1 + \rho_F\xi_3\varepsilon_1 + \xi_2$, and $\omega_5(a,b,c,f) = \int_0^\infty \frac{1}{ax+b}e^{-\left(cx^2+fx\right)}dx$. By utilizing [32, (10), (11)], [33, (6.2.8)], and [34, (2.3)], we obtain

$$
\begin{aligned}
\omega_5(a,b,c,f) &= \frac{1}{b}\int_0^\infty H_{0,1}^{1,0}\left[fx\,\Big|\,_{(0,1)}^{-}\right] H_{1,1}^{1,1}\left[\frac{a}{b}x\,\Big|\,_{(0,1)}^{(0,1)}\right] H_{0,1}^{1,0}\left[cx^2\,\Big|\,_{(0,1)}^{-}\right] dx \\
&= \frac{f^{N-1}}{b}H_{1,0:1,1:0,1}^{1,0:1,1:1,0}\left[_{-}^{(0;1,2)}\,\Big|\,_{(0,1)}^{(0,1)}\,\Big|\,_{(0,1)}^{-}\,\Big|\,\frac{a}{bf},\frac{c}{f^2}\right].
\end{aligned}
$$

(E.15)

With the same method, we obtain

$$
\begin{aligned}
I_4 &= \int_0^\infty f_{|H_E|^2}(t)\, dt \int_{(\rho_F t+1)\varepsilon_1}^{\infty} f_{|h_B|^2}(s)\, F_{|h_k|^2,|h_{k+1}|^2|h_K|^2}\left(0,\alpha_{th}+\theta_{th}t,\frac{\tau_B}{\rho_F},\omega_0(s,t)\right) ds \\
&= \sum_{n=0}^{K-k-2}\sum_{m=0}^{k-1}\sum_{i=1}^{6}\varsigma_i \int_0^\infty \int_{(\rho_F t+1)\varepsilon_1}^{\infty} e^{-B_i(\alpha_{th}+\theta_{th}t)-C_i\frac{\tau_B}{\rho_F}-W_i\omega_0(s,t)} f_{|h_B|^2}(s)\, f_{|H_E|^2}(t)\, ds dt \\
&= r_B^\alpha r_E^{N\alpha}\sum_{n=0}^{K-k-2}\sum_{m=0}^{k-1}\left(\sum_{i=1}^{4}\frac{\varsigma_i e^{-\xi_4}}{\Gamma(N)}\Delta_3 + \sum_{i=5}^{6}\varsigma_i e^{-\xi_4}\Delta_4\right),
\end{aligned}
$$

(E.16)

where $\xi_4 = (B_i+W_i)\alpha_{th} - \frac{C_i}{\rho_F}$, $\Delta_3 = \frac{e^{-\xi_6\varepsilon_1}\omega_6(u_1,\xi_6,v_2,l_2)}{\Gamma(N)}$, $\Delta_4 = \frac{e^{-\xi_6\varepsilon_1}}{\xi_6(\rho_F\xi_6\varepsilon_1+\xi_5)^N}$, $v_2 = u_1\rho_F\varepsilon_1$, $l_2 = u_1\varepsilon_1 + \xi_6\rho_F\varepsilon_1 + \xi_5$, $\xi_5 = (B_i+W_i)\theta_{th}+r_E^\alpha$, and $\xi_6 = W_i\alpha_{th}\rho_B + \frac{C_i}{P_F\alpha_B}+r_B^\alpha$.

Similar to (E.11) and (E.12), we obtain

$$
\Pr\left\{|\mathcal{S}_{\mathrm{II}}| = K-1, |h_B|^2 > \alpha_B\right\} = \Pr\left\{|h_{K-1}|^2 < \frac{\tau_B}{\rho_F} < |h_K|^2, |h_B|^2 > \alpha_B\right\}
$$

(E.17)

and

$$
\begin{aligned}
&\Pr\left\{\max\left\{R_K^{\mathrm{I}}, R_{K-1}^{\mathrm{II}}\right\} - R_E < R_{th}\right\} \\
&= \Pr\left\{|h_{K-1}|^2 < \theta_{th}|H_E|^2 + \alpha_{th}, |h_K|^2 < \omega_0\left(|h_B|^2, |H_E|^2\right)\right\}.
\end{aligned}
$$

(E.18)

Then, $P_{out,3}^{K-1}$ is obtained as

$$
\begin{aligned}
P_{out,3}^{K-1} &= \Pr\left\{R_{K-1}^s < R_{th}, |\mathcal{S}_{\mathrm{II}}| = K - 1, |h_B|^2 > \alpha_B\right\} \\
&= \Pr\left\{|h_{K-1}|^2 < \frac{\tau_B}{\rho_F} < |h_K|^2 < \omega_0\left(|h_B|^2, |H_E|^2\right), \alpha_B < |h_B|^2 < \left(\rho_F|H_E|^2 + 1\right)\varepsilon_1\right\} \\
&+ \Pr\left\{|h_{K-1}|^2 < \theta_{th}|H_E|^2 + \alpha_{th}, \frac{\tau_B}{\rho_F} < |h_K|^2 < \omega_0\left(|h_B|^2, |H_E|^2\right), |h_B|^2 > \left(\rho_F|H_E|^2 + 1\right)\varepsilon_1\right\} \\
&= \int_0^\infty f_{|H_E|^2}(t)\,dt \int_{\alpha_B}^{(\rho_F t+1)\varepsilon_1} f_{|h_B|^2}(s)\,F_{|h_{K-1}|^2,|h_K|^2}\left(0, \frac{\tau_B}{\rho_F}, \frac{\tau_B}{\rho_F}, \omega_0(s,t)\right)\,ds \\
&+ \int_0^\infty f_{|H_E|^2}(t)\,dt \int_{(\rho_F t+1)\varepsilon_1}^{\infty} f_{|h_B|^2}(s)\,F_{|h_{K-1}|^2,|h_K|^2}\left(0, \theta_{th}t + \alpha_{th}, \frac{\tau_B}{\rho_F}, \omega_0(s,t)\right)\,ds \\
&= r_B^\alpha r_E^{N\alpha} \sum_{n=0}^{K-2} \frac{\mu_0}{C_0}\left(\sum_{j=1}^{2} \frac{(-1)^{j+1}}{\Gamma(N)}\left(e^{-\zeta_1}\Delta_5 + e^{-\zeta_4}\Delta_7\right) + \sum_{j=3}^{4}(-1)^{j+1}\left(e^{-\zeta_1}\Delta_6 + e^{-\zeta_4}\Delta_8\right)\right),
\end{aligned}
$$

$$(\text{E.19})$$

where $\zeta_1 = q_j\alpha_{th} - \frac{b_j + c_j}{\rho_F}$, $\zeta_2 = q_j\theta_{th} + r_E^\alpha$, $\zeta_3 = q_j\alpha_{th}\rho_B + \frac{b_j + c_j}{P_F\alpha_B} + r_B^\alpha$, $\Delta_5 = \frac{\zeta_3^{N-1}}{u_2^N}e^{\frac{\zeta_2\zeta_3}{u_2}}\Gamma\left(1 - N, \zeta_3\alpha_B + \frac{\zeta_2\zeta_3}{u_2}\right)$ $- \frac{e^{-\xi_3\varepsilon_1}\omega_5(u_2,\zeta_3,v_3,l_3)}{\Gamma(N)}$, $u_2 = q_j\rho_B\theta_{th}$, $v_3 = u_2\rho_F\varepsilon_1$, $l_3 = u_2\varepsilon_1 + \zeta_3\rho_F\varepsilon_1 + \zeta_2$, $\Delta_6 = \frac{e^{-\zeta_3\alpha_B}}{\zeta_2^N\zeta_3} - \frac{e^{-\zeta_3\varepsilon_1}}{\zeta_3(P_F\zeta_3\varepsilon_1 + \zeta_2)^N}$, $\zeta_4 = (b_j + q_j)\alpha_{th} - \frac{c_i}{\rho_F}$, $\zeta_5 = (b_j + q_j)\theta_{th} + r_E^\alpha$, $\zeta_6 = q_i\alpha_{th}\rho_B + \frac{c_j}{P_F\alpha_B} + r_B^\alpha$, $\Delta_7 = \frac{e^{-\zeta_6\varepsilon_1}\omega_5(u_2,\zeta_6,v_4,l_4)}{\Gamma(N)}$, $v_4 = u_2\rho_F\varepsilon_1$, $l_4 = u_2\varepsilon_1 + \zeta_6\rho_F\varepsilon_1 + \zeta_5$, and $\Delta_8 = \frac{e^{-\zeta_6\varepsilon_1}}{\zeta_6(\rho_F\zeta_6\varepsilon_1 + \zeta_5)^N}$.

APPENDIX F

PROOF OF COROLLARY 4

When $\rho_F = \rho_B \to \infty$, we have $\alpha_B \to 0, \alpha_{th} \to 0$. One can obtain $P_{out,1}^{1,\infty} \approx 0$ due to $\Pr\left\{|h_B|^2 < \alpha_B\right\} \approx 0$. Based on (E.3) and (E.4), $P_{out,1}^2$ is approximated as

$$
\begin{aligned}
P_{out,1}^{2,\infty} &\approx \Pr\left\{\frac{|h_B|^2}{\varepsilon_B} < |h_1|^2 < |h_K|^2 < \omega_0\left(|h_B|^2, |H_E|^2\right)\right\} \\
&= \int_0^\infty \int_0^\infty \left(F_{|h_1|^2,|h_K|^2}\left(\frac{x}{\varepsilon_B}, \omega_0(x,y)\right)\right) f_{|h_B|^2}(x)\,dx\,f_{|H_E|^2}(y)\,dy \\
&\overset{(g)}{\approx} \sum_{n=0}^{K-2} \frac{\varepsilon_B\mu_1}{K\left(\frac{r_E}{r_B}\right)^\alpha + \varepsilon_B},
\end{aligned}
$$

$$(\text{F.1})$$

where (g) holds with the same method as (f).

Based on (E.8) and (E.9), $P_{out,2}$ is approximated as

$$
\begin{aligned}
P_{out,2}^{\infty} &\approx \Pr\left\{|h_K|^2 < \theta_{th}|H_E|^2, |h_B|^2 > \varepsilon_B|H_E|^2\right\} \\
&\quad + \Pr\left\{|h_K|^2 < \frac{|h_B|^2}{\varepsilon_B}, |h_B|^2 < \varepsilon_B|H_E|^2\right\} \\
&= \frac{r_B^{\alpha} r_E^{N\alpha}}{\Gamma(N)} \sum_{i=0}^{K} \varphi_i \int_0^{\infty} y^{N-1} e^{-\left(i r_F^{\alpha}\theta_{th}+r_E^{\alpha}\right)y} \int_{\varepsilon_B\theta_{th}y}^{\infty} e^{-r_B^{\alpha}x} dxdy \\
&\quad + \frac{r_B^{\alpha} r_E^{N\alpha}}{\Gamma(N)} \sum_{i=0}^{K} \varphi_i \int_0^{\infty} y^{N-1} e^{-r_E^{\alpha}y} \int_0^{\varepsilon_B\theta_{th}y} e^{-\left(\frac{i r_F^{\alpha}}{\varepsilon_B}+r_E^{\alpha}\right)x} dxdy \\
&= \sum_{i=0}^{K} \frac{\varphi_i\varepsilon_B}{i\left(\frac{r_F}{r_B}\right)^{\alpha}+\varepsilon_B} + \sum_{i=0}^{K} \frac{i\varphi_i(i\chi_1+\chi_2)^{-N}}{i+\varepsilon_B\left(\frac{r_B}{r_F}\right)^{\alpha}},
\end{aligned}
$$

(F.2)

where $\chi_1 = \theta_{th}\left(\frac{r_F}{r_E}\right)^{\alpha}$ and $\chi_2 = \varepsilon_B\theta_{th}\left(\frac{r_B}{r_E}\right)^{\alpha}+1$.

Based on (E.13), we obtain

$$
\begin{aligned}
I_3^{\infty} &\approx \Pr\left\{|h_k|^2 < \frac{|h_B|^2}{\varepsilon_B} < |h_{k+1}|^2 < |h_K|^2 < \omega_0\left(|h_B|^2, |H_E|^2\right), |h_B|^2 < \varepsilon_B\theta_{th}|H_E|^2\right\} \\
&= \sum_{n=0}^{K-k-2} \sum_{m=0}^{k-1} \sum_{i=1}^{6} \varsigma_i \int_0^{\infty} \int_0^{\varepsilon_B\theta_{th}t} e^{-(B_i+C_i)\frac{s}{\varepsilon_B}-W_i\omega_0(s,t)} f_{|h_B|^2}(s) f_{|H_E|^2}(t)\, dsdt \\
&\overset{(h)}{=} \sum_{n=0}^{K-k-2} \sum_{m=0}^{k-1} \sum_{i=5}^{6} \frac{\varsigma_i\varepsilon_B(1-\chi_3)}{(K+\varpi_i)\left(\frac{r_F}{r_B}\right)^{\alpha}+\varepsilon_B},
\end{aligned}
$$

(F.3)

and

$$
\begin{aligned}
I_4^{\infty} &\approx \Pr\left\{|h_k|^2 < \theta_{th}|H_E|^2, \frac{|h_B|^2}{\varepsilon_B} < |h_{k+1}|^2 < |h_K|^2 < \omega_0\left(|h_B|^2, |H_E|^2\right), |h_B|^2 > \varepsilon_B\theta_{th}|H_E|^2\right\} \\
&= \sum_{n=0}^{K-k-2} \sum_{m=0}^{k-1} \sum_{i=1}^{6} \varsigma_i \int_0^{\infty} \int_{\varepsilon_B\theta_{th}t}^{\infty} e^{-B_i\theta_{th}t-C_i\frac{s}{\varepsilon_B}-W_i(\omega_0(s,t))} f_{|h_B|^2}(s) f_{|H_E|^2}(t)\, dsdt \\
&\overset{(i)}{=} \sum_{n=0}^{K-k-2} \sum_{m=0}^{k-1} \sum_{i=5}^{6} \frac{\varsigma_i\varepsilon_B\chi_3}{\left((K-k)\left(\frac{r_F}{r_B}\right)^{\alpha}+\varepsilon_B\right)},
\end{aligned}
$$

(F.4)

where $\chi_3 = \left((K+\varpi_i)\chi_1+\chi_2\right)^{-N}$, (h) and (i) hold with the same method as (f), and $\varpi = [0,0,n+2,1,m+1-k,-k]$.

Thus, $P_{out,3}^k$, when $\rho_F = \rho_B \to \infty$, is approximated as

$$
P_{out,3}^{k,\infty} = \sum_{k=1}^{K-2} \left(I_3^{\infty} + I_4^{\infty}\right).
$$

(F.5)

With the same method and based on (E.19), $P_{out,3}^{K-1}$ is approximated as

$$
\begin{aligned}
P_{out,3}^{K-1,\infty} &\approx \Pr\left\{R_{K-1}^s < R_{th}, |S_{\mathrm{II}}| = K-1\right\} \\
&= \Pr\left\{|h_{K-1}|^2 < \frac{|h_B|^2}{\varepsilon_B} < |h_K|^2 < \omega_0\left(|h_B|^2, |H_E|^2\right), |h_B|^2 < \varepsilon_B\theta_{th}|H_E|^2\right\} \\
&\quad + \Pr\left\{|h_{K-1}|^2 < \theta_{th}|H_E|^2, \frac{|h_B|^2}{\varepsilon_B} < |h_K|^2 < \omega_0\left(|h_B|^2, |H_E|^2\right), |h_B|^2 > \varepsilon_B\theta_{th}|H_E|^2\right\} \\
&= \int_0^\infty f_{|H_E|^2}(t)\, dt \int_0^{\varepsilon_B\theta_{th}t} f_{|h_B|^2}(s)\, F_{|h_{K-1}|^2,|h_K|^2}\left(0, \frac{s}{\varepsilon_B}, \frac{s}{\varepsilon_B}, \omega_0(s,t)\right) ds \\
&\quad + \int_0^\infty f_{|H_E|^2}(t)\, dt \int_{\varepsilon_B\theta_{th}t}^\infty f_{|h_B|^2}(s)\, F_{|h_{K-1}|^2,|h_K|^2}\left(0, \theta_{th}t, \frac{s}{\varepsilon_B}, \omega_0(s,t)\right) ds \\
&\overset{(j)}{=} \sum_{n=0}^{K-2} \mu_4 \sum_{j=3}^{4} (-1)^{j+1}\varepsilon_B\left(\frac{1-\chi_4}{\varpi_j r_B^{-\alpha} + r_F^{-\alpha}\varepsilon_B} + \frac{\chi_4}{r_B^{-\alpha} + r_F^{-\alpha}\varepsilon_B}\right),
\end{aligned}
$$

$$(F.6)$$

where $\mu_4 = \frac{K!(-1)^n\binom{K-2}{n}}{(K-2)!(n+1)}$, $\chi_4 = (\varpi_j\chi_1 + \chi_2)^{-N}$, and (j) holds with the same method as (f).

References

[1] W. Jiang, B. Han, M. A. Habibi, and H. D. Schotten, "The road towards 6G: A comprehensive survey," *IEEE Open J. Commun. Soc.*, vol. 2, pp. 334-366, Feb. 2021.

[2] M. Shirvanimoghaddam, M. S. Mohammadi, R. Abbas, A. Minja, C. Yue, B. Matuz, G. Han, Z. Lin, W. Liu, Y. Li, S. Johnson, and B. Vucetic, "Short block-length codes for ultra-reliable low latency communications," *IEEE Commun. Mag.*, vol. 57, no. 2, pp. 130-137, Feb. 2019.

[3] M. El-Tanab and W. Hamouda, "An overview of uplink access techniques in machine-type communications," *IEEE Netw.*, vol. 35, no. 3, pp. 246-251, May 2021.

[4] *UL Grant-Free Transmission for URLLC*, document R1-1705654, 3GPP TSG-RAN WG1 #88, Apr. 2017.

[5] Z. Ma, M. Xiao, Y. Xiao, Z. Pang, H. V. Poor, and B. Vucetic, "High-reliability and low-latency wireless communication for internet of things: Challenges, fundamentals and enabling technologies," *IEEE Internet Things J.*, vol. 6, no. 5, pp. 7946-7970, Oct. 2019.

[6] J. Zhang, X. Tao, H. Wu, N. Zhang, and X. Zhang, "Deep reinforcement learning for throughput improvement of the uplink grant-free NOMA system," *IEEE Internet Things J.*, vol. 7, no. 7, pp. 6369-6379, Jul. 2020.

[7] Z. Ding, X. Lei, G. K. Karagiannidis, R. Schober, J. Yuan, and V. K. Bhargava, "A survey on non-orthogonal multiple access for 5G networks: Research challenges and future trends," *IEEE J. Sel. Areas Commun.*, vol. 35, no. 10, pp. 2181-2195, Oct. 2017.

[8] M. B. Shahab, R. Abbas, M. Shirvanimoghaddam, and S. J. Johnson, "Grant-free non-orthogonal multiple access for IoT: A survey," *IEEE Commun. Surveys Tuts.*, vol. 22, no. 3, pp. 1805-1838, 3nd Quar. 2020.

[9] R. Abbas, M. Shirvanimoghaddam, Y. Li, and B. Vucetic, "A novel analytical framework for massive grant-free NOMA," *IEEE Trans. Commun.*, vol. 67, no. 3, pp. 2436-2449, Mar. 2019.

[10] J. Chen, L. Guo, J. Jia, J. Shang, and X. Wang, "Resource allocation for IRS assisted SGF NOMA transmission: A MADRL approach," *IEEE J. Sel. Areas Commun.*, vol. 40, no. 4, pp. 1302-1316, Apr. 2022.

[11] K. Yang, N. Yang, N. Ye, M. Jia, Z. Gao, and R. Fan, "Non-orthogonal multiple access: Achieving sustainable future radio access," *IEEE Commun. Mag.*, vol. 57, no. 2, pp. 116-121, Feb. 2019.

[12] Z. Ding, R. Schober, P. Fan, and H. V. Poor, "Simple semi-grant-free transmission strategies assisted by non-orthogonal multiple access," *IEEE Trans. Commun.*, vol. 67, no. 6, pp. 4464-4478, Jun. 2019.

[13] Z. Yang, P. Xu, J. Ahmed Hussein, Y. Wu, Z. Ding, and P. Fan, "Adaptive power allocation for uplink non-orthogonal multiple access with semi-grant-free transmission," *IEEE Wireless Commun. Lett.*, vol. 9, no. 10, pp. 1725-1729, Oct. 2020.

[14] C. Zhang, Y. Liu, W. Yi, Z. Qin, and Z. Ding, "Semi-grant-free NOMA: Ergodic rates analysis with randomly deployed users," *IEEE Wireless Commun. Lett.*, vol. 10, no. 4, pp. 692-695, Apr. 2021.

[15] C. Zhang, Y. Liu, and Z. Ding, "Semi-grant-free NOMA: A stochastic geometry model," *IEEE Trans. Wireless Commun.*, vol. 21, no. 2, pp. 1197-1213, Feb. 2022.

[16] Z. Ding, R. Schober, and H. V. Poor. "A new QoS-guarantee strategy for NOMA assisted semi-grant-free transmission," *IEEE Trans. Commun.*, vol. 69, no. 11, pp. 7489-7503, Nov. 2021.

[17] Y. Sun, Z. Ding, and X. Dai, "A new design of hybrid SIC for improving transmission robustness in uplink NOMA," *IEEE Trans. Veh. Technol.*, vol. 70, no. 5, pp. 5083-5087, May 2021.

[18] H. Lu, *et al*. "Advanced NOMA assisted semi-grant-free transmission schemes for randomly distributed users," *IEEE Trans. Wireless Commun.*, doi: 10.1109/TWC.2022.3227555, 2022.

[19] Y. Liu, Z. Qin, M. Elkashlan, Y. Gao, and L. Hanzo, "Enhancing the physical layer security of NOMA in large-scale networks," *IEEE Trans. Wireless Commun.*, vol. 16, no. 3, pp. 1656–1671, Mar. 2017.

[20] B. He, A. Liu, N. Yang, and V. K. N. Lau, "On the design of secure non-orthogonal multiple access systems," *IEEE J. Sel. Areas Commun.*,vol. 35, no. 10, pp. 2196–2206, Oct. 2017.

[21] L. Lv, F. Zhou, J. Chen, and N. Al-Dhahir, "Secure cooperative communications with an untrusted relay: A NOMA-inspired jamming and relaying approach," *IEEE Trans. Inf. Forensics Security*, vol. 14, no. 12, pp. 3191–3205, Apr. 2019.

[22] H. Lei, Z. Yang, K.-H. Park, I. S. Ansari, Y. Guo, G. Pan, and M.-S. Alouini, "Secrecy outage analysis for cooperative NOMA systems with relay selection schemes," *IEEE Trans. Commun.*, vol. 67, no. 9, pp. 6282-6298, Sept. 2019.

[23] H.-M. Wang and X. Zhang, "UAV secure downlink NOMA transmissions: A secure users oriented perspective," *IEEE Trans. Commun.*, vol. 68, no. 9, pp. 5732-5746, Sept. 2020.

[24] N. Zhao, Y. Li, S. Zhang, Y. Chen, W. Lu, J. Wang, and X. Wang, "Security enhancement for NOMA-UAV networks," *IEEE Trans. Veh. Technol.*, vol. 69, no. 4, pp. 3994–4005, Apr. 2020.

[25] H. Lei, R. Gao, K.-H. Park, I. S. Ansari, K. J. Kim, and M.-S. Alouini, "On secure downlink NOMA systems with outage constraint," *IEEE Trans. Commun.*, vol. 68, no. 12, pp. 7824-7836, Dec. 2020.

[26] K. Wang, H. Li, Z. Ding, and P. Xiao, "Reinforcement learning based latency minimization in secure NOMA-MEC systems with hybrid SIC," *IEEE Trans. Wireless Commun.*, vol. 22, no. 1, pp. 408-422, Jan. 2023.

[27] Z. Ding, R. Schober, and H. V. Poor, "Unveiling the importance of SIC in NOMA systems—Part II: New results and future directions," *IEEE Commun. Lett.*, vol. 24, no. 11, pp. 2378-2382, Nov. 2020.

[28] M. Bloch, J. Barros, M. R. D. Rodrigues, and S. W. McLaughlin, "Wireless information-theoretic security," *IEEE Trans. Inf. Theory*, vol. 54, no. 6, pp. 2515-2534, Jun. 2008.

[29] H. Lei, I. S. Ansari, G. Pan, B. Alomair, and M.-S. Alouini, "Secrecy capacity analysis over α-μ fading channels," *IEEE Commun. Lett.*, vol. 21, no. 6, pp. 1445-1448, Jun. 2017.

[30] I. S. Gradshteyn and I. M. Ryzhik, *Table of Integrals, Series, and Products*, 7th edition. Academic Press, 2007.

[31] M. Abramowitz and I. Stegun, *Handbook of Mathematical Functions With Formulas, Graphs, and Mathematical Tables*, 9th. New York, NY, USA: Discover, 1972.

[32] V. S. Adamchik and O. I. Marichev, "The algorithm for calculating integrals of hypergeometric type functions and its realization in REDUCE system," in *Proc. the international symposium on Symbolic and algebraic computation (ISSAC '90)*, Tokyo, Japan, Aug. 1990, pp. 212-224.

[33] M. D. Springer, *The Algebra of Random Variables*. New York: Wiley 1979.

[34] P. K. Mittal and K. C. Gupta, "An integral involving the generalized function of two variables," *Proceedings of the Indian Academy of Sciences - Section A*, vol. 75, no. 3, pp. 117-123, Mar. 1972.

[35] J. Choi, J. Ding, N.-P. Le, and Z. Ding, "Grant-free random access in machine-type communication: Approaches and challenges," *IEEE Wireless Commun.*, vol. 29, no. 1, pp. 151-158, 2022.

[36] Z. Ding, R. Schober, P. Fan, and H. V. Poor, "Simple semi-grant-free transmission strategies assisted by non-orthogonal multiple access," *IEEE Trans. Commun.*, vol. 67, no. 6, pp. 4464-4478, Jun. 2019.

[37] S. Verdu, *Multiuser Detection*. Cambridge University Press, Cambridge, UK, 1998.